Probing Nuclear Structure at the Ultra-Relativistic Heavy-Ion Collisions

Zhiyong Lu

China Institute of Atomic Energy, Beijing, China

8—Aug—2024

Nuclear structure at low energies

Atomic nuclei have rich phenomenology. Rooted in the strong nuclear force.
Nuclear structure is a very old field. Many different approaches.

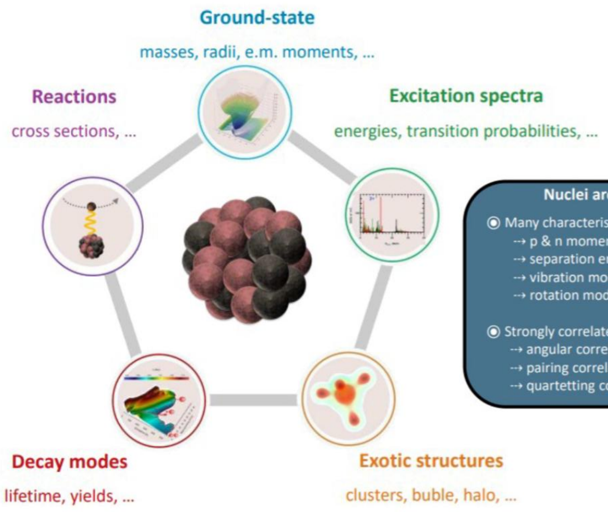

Nuclei are complex systems

- Many characteristic scales :
  - ⇢ p & n momenta ~ 100 MeV
  - ⇢ separation energies ~ 10 MeV
  - ⇢ vibration modes ~ 1MeV
  - ⇢ rotation modes ~ 0.01-5 MeV
- Strongly correlated:
  - ⇢ angular correlations ⇒ deformation
  - ⇢ pairing correlations ⇒ superfluidity
  - ⇢ quartetting correlations ⇒ clustering

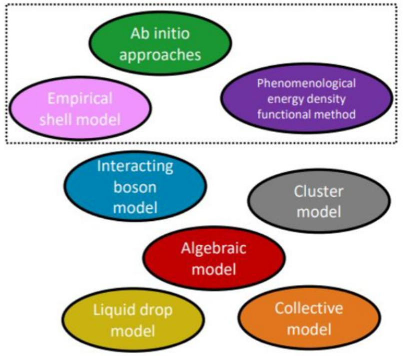

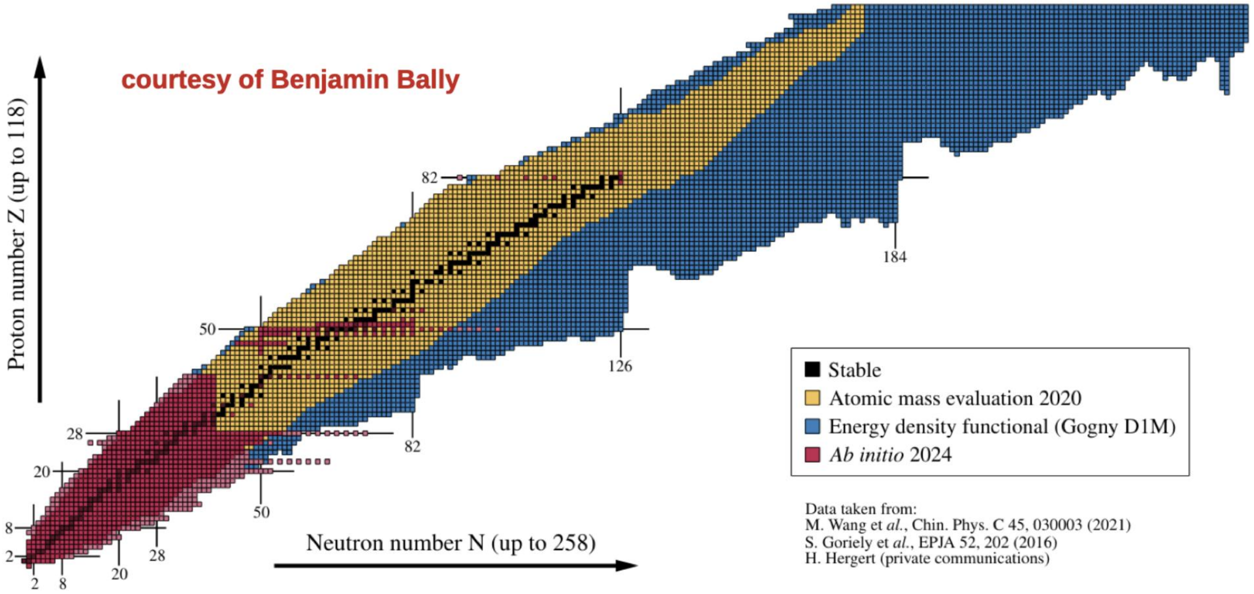

Modern ab-initio methods have successfully described light nuclei with A $\lesssim$ 50

- *there are no real probes of multi-nucleon correlations*
- *huge model dependence.*

For heavy nuclei, computational complexity rapidly arises due to the increasing number of nucleons

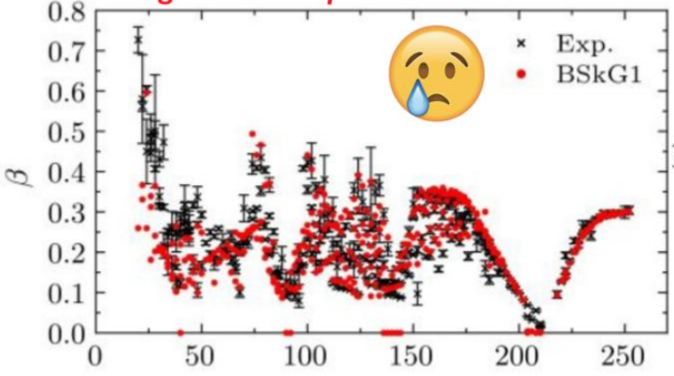

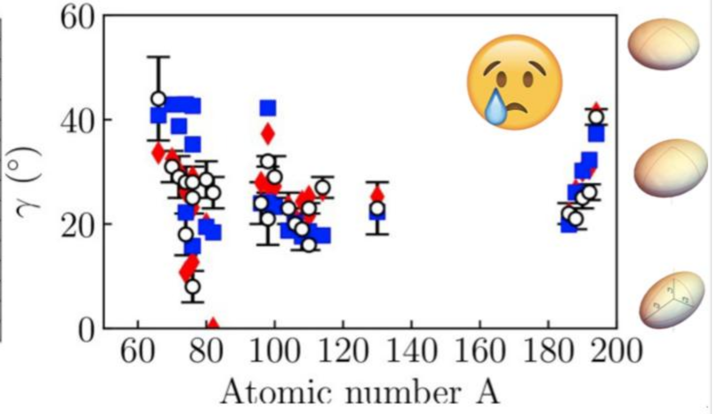

Nuclear structure at high energies

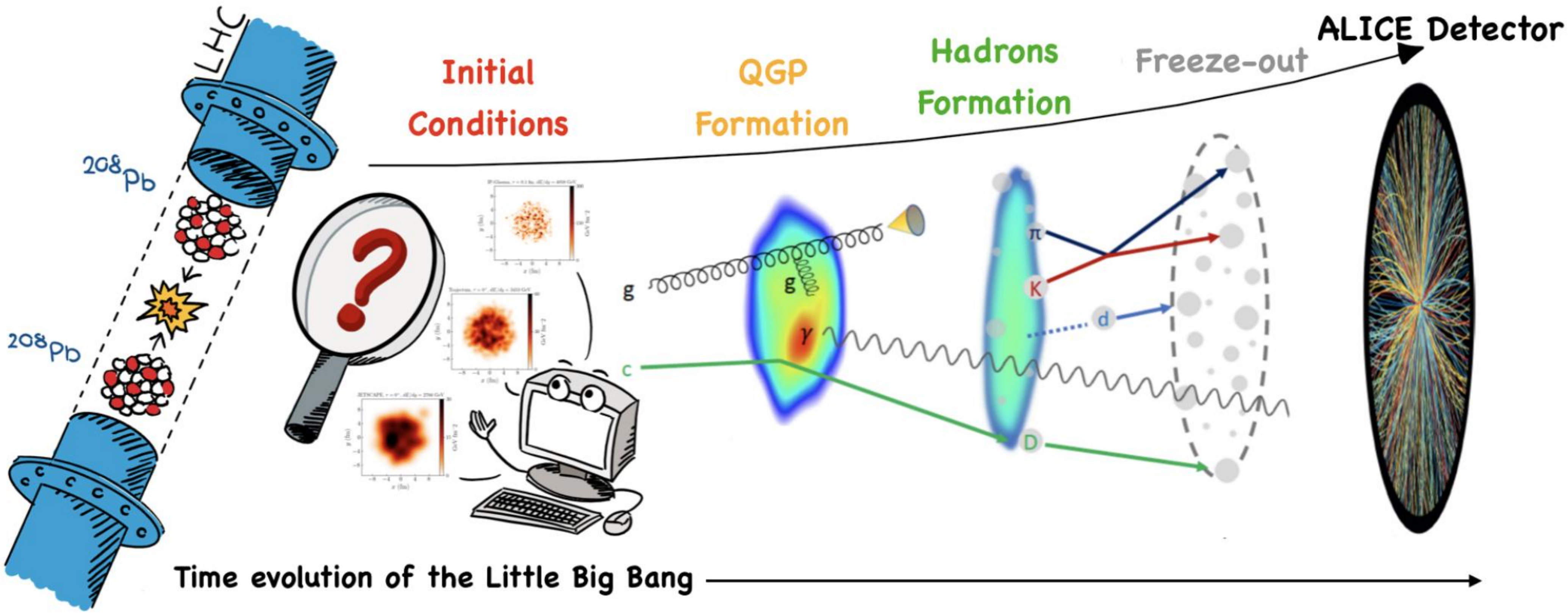

system expansion

nuclear structure ⟷ **inital conditions** ⇄ **azimuthal distribution of final-state particles**

probe

From final state to nuclear structure

nucleon density described by **Woods-Saxon profile**

$$\rho(r,\theta,\phi) = \frac{\rho_0}{1+e^{[r-R(\theta,\phi)]/a_0}},$$
$$R(\theta,\phi) = R_0(1+\beta_2[\cos\gamma Y_{2,0}+\sin\gamma Y_{2,2}]),$$

β_2: overall deformation parameter
a_0: diffuseness parameter

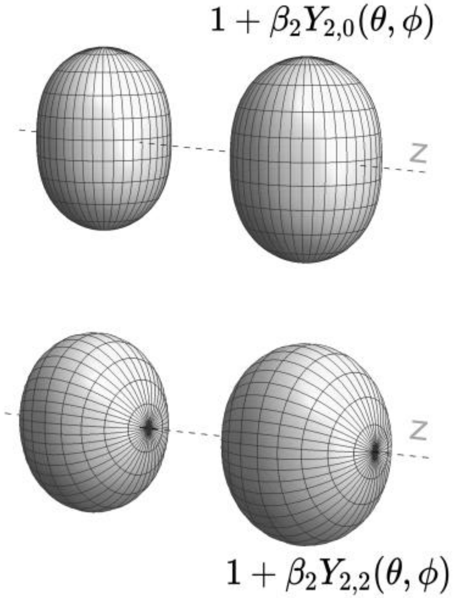

Radial profile:

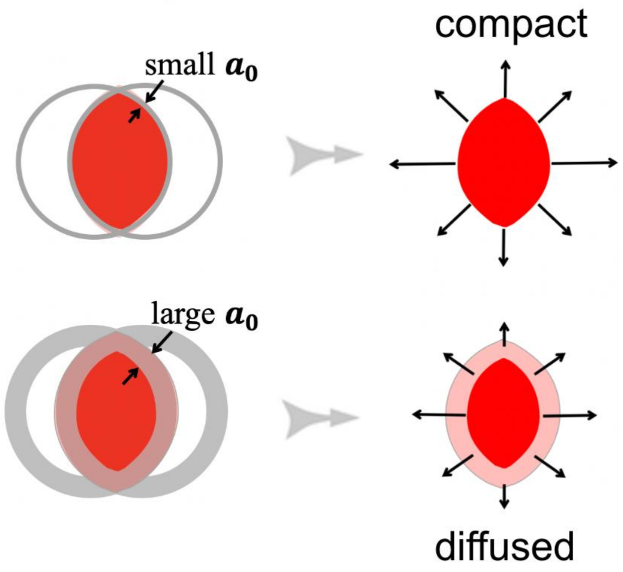

From final state to nuclear structure

nucleon density described by **Woods-Saxon profile**

$$\rho(r,\theta,\phi) = \frac{\rho_0}{1+e^{[r-R(\theta,\phi)]/a_0}},$$

$$R(\theta,\phi) = R_0(1+\beta_2[\cos\gamma Y_{2,0} + \sin\gamma Y_{2,2}]),$$

γ: traxiality parameter

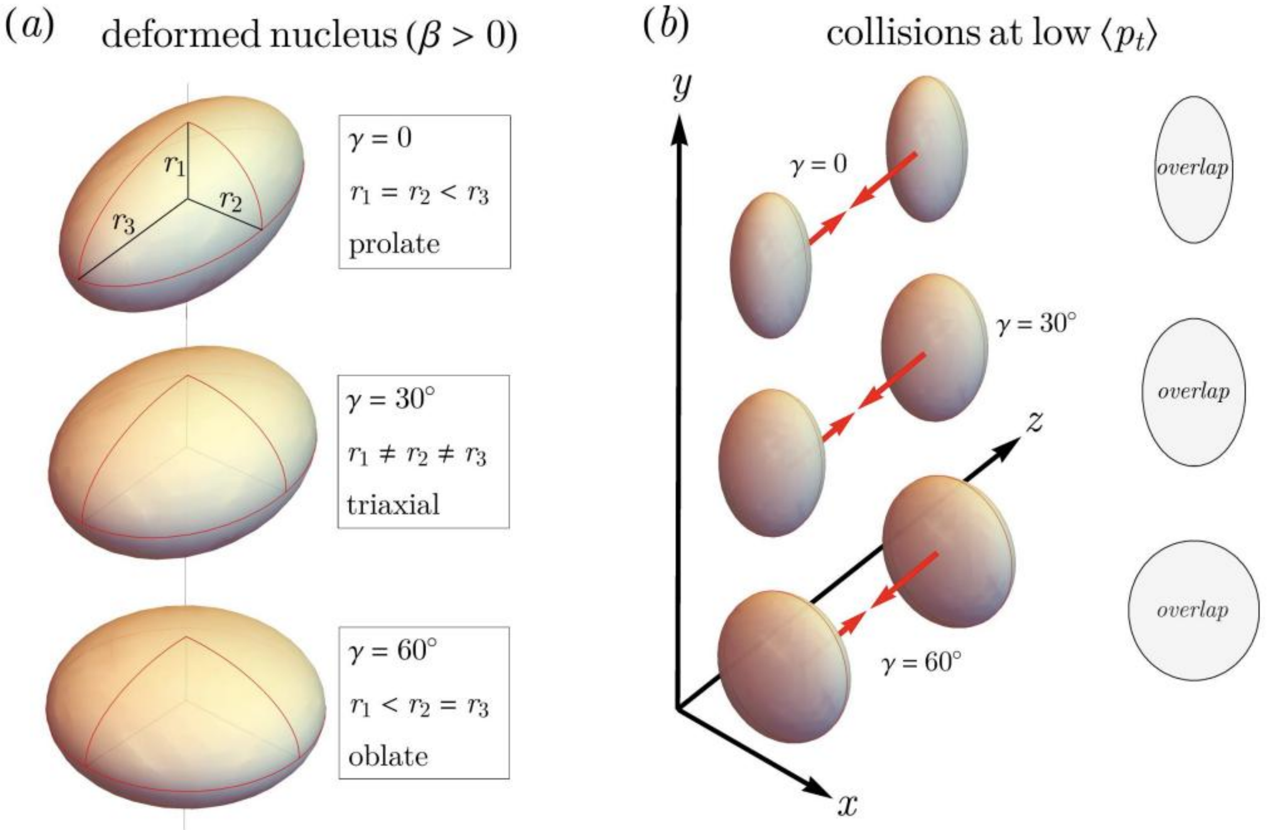

From final state to nuclear structure

Most of nuclear structure studies on GeV energies are inplemented in the isobar runs of $^{96}Ru+^{96}Ru$ and $^{96}Zr+^{96}Zr$ in RHIC

J. Jia, Phys. Rev. Lett. 131 no. 2, (2023) 022301
J. Jia, Chin. Phys. Lett. 40 no. 4, (2023) 042501
S. Zhao, Phys. Lett. B 839 (2023) 137838
etc...

β_2=0.2, γ=30°

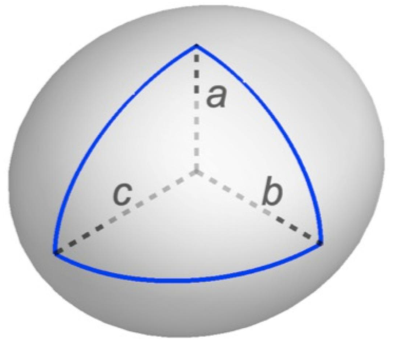

$a \neq b \neq c$

J. Jia, Phys.Rev.C 105 (2022) 4, 044905

At the LHC, B. Bally et al., Phys.Rev.Lett. 128 (2022) 8, 082301

^{129}Xe is predicted to have deformed and triaxial structure ($r_1 \neq r_2 \neq r_3$).

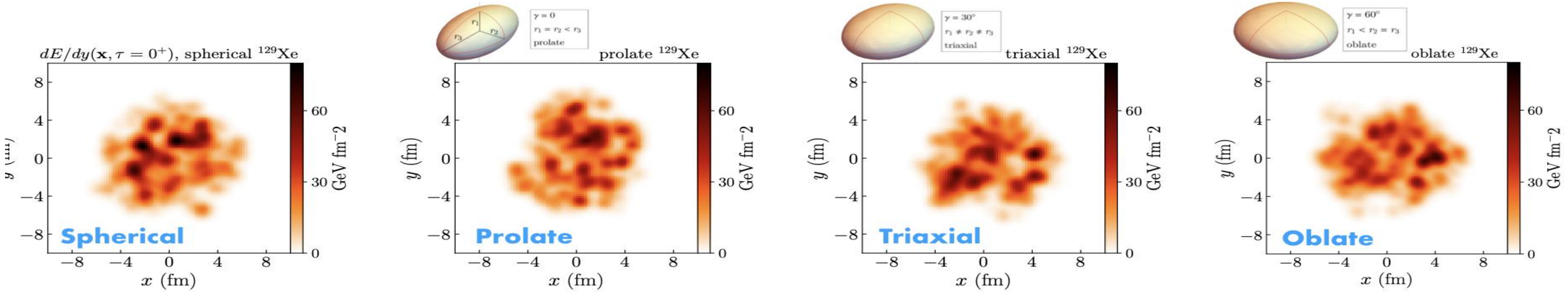

Centrality determination

A very important value in NS at high energies

Centrality: a percentage of the hadronic cross section corresponding to a particle multiplicity, directly related to the impact parameter

0% centrality: almost fully overlap
90% centrality: peripheral collisions

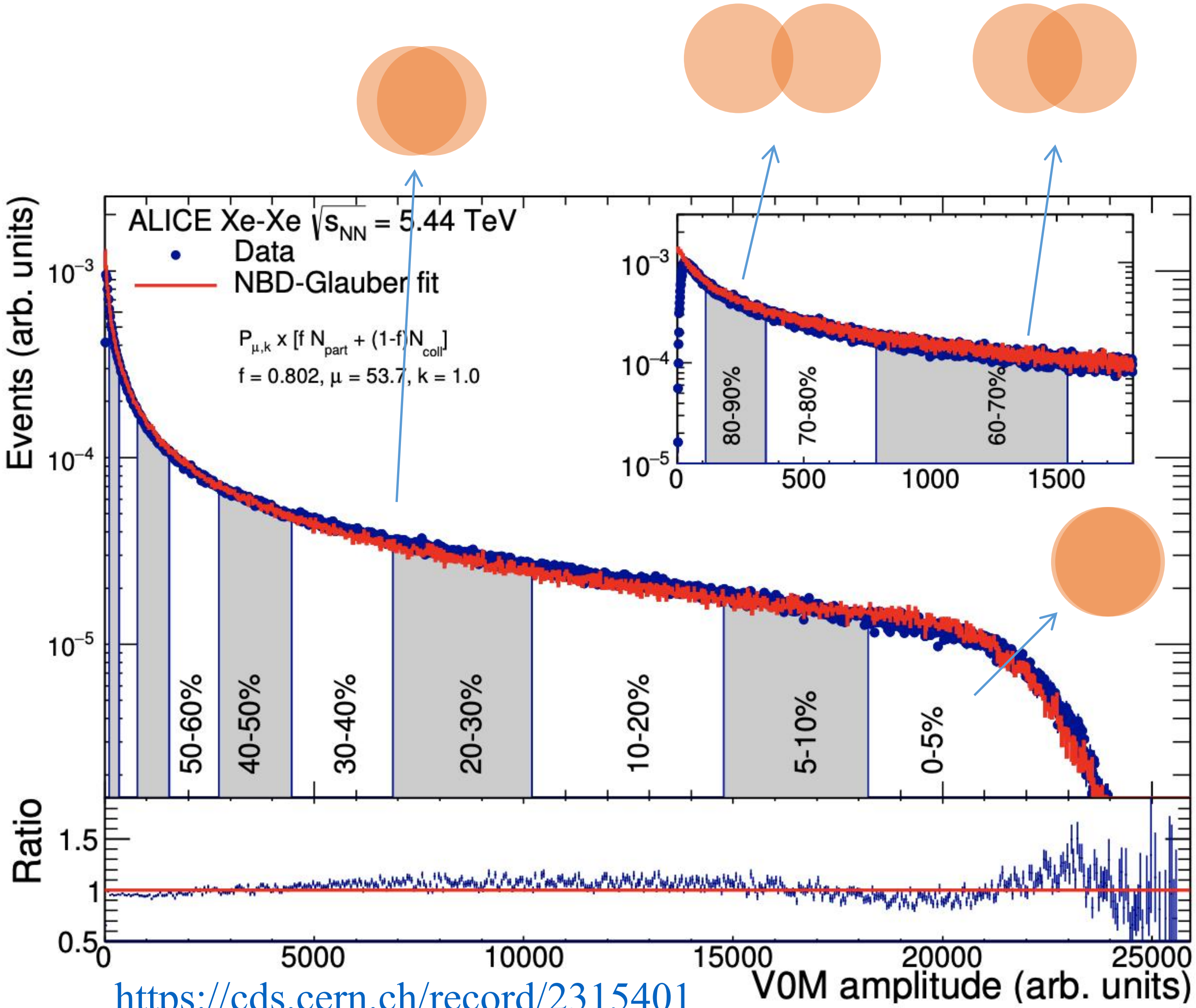

https://cds.cern.ch/record/2315401

ALICE detector and data sample

1. Inner Tracking System (ITS)
- Tracking and triggering

2. V0 detector
- Triggering and event
- centrality determination

3. Time Projection Chamber (TPC)
- Tracking

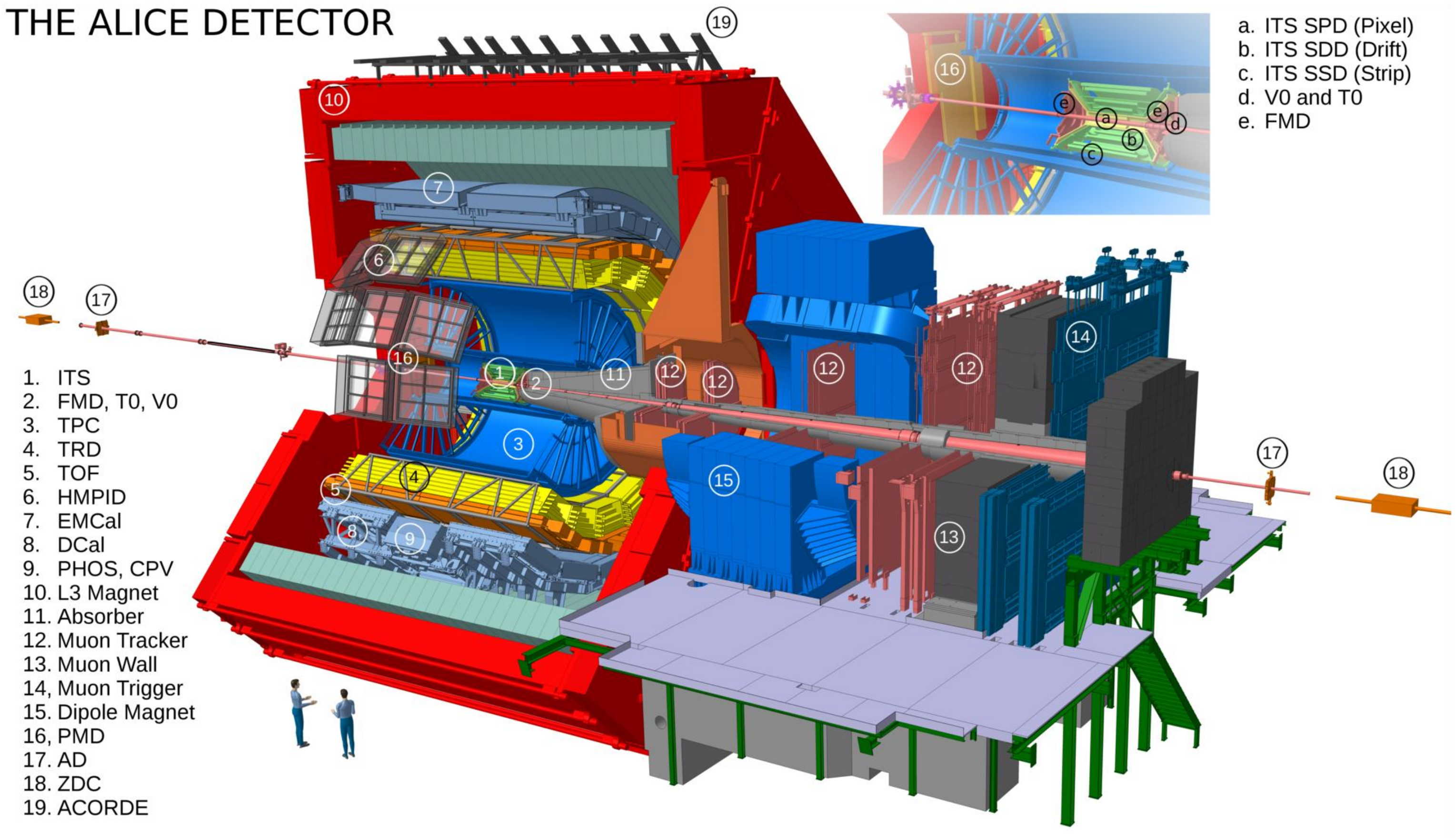

Kinematic region:
$0.2 < p_{\mathrm{T}} < 3.0$ GeV/c
$|\eta| < 0.8$

Anisotropic flow

anisotropic pressure gradients

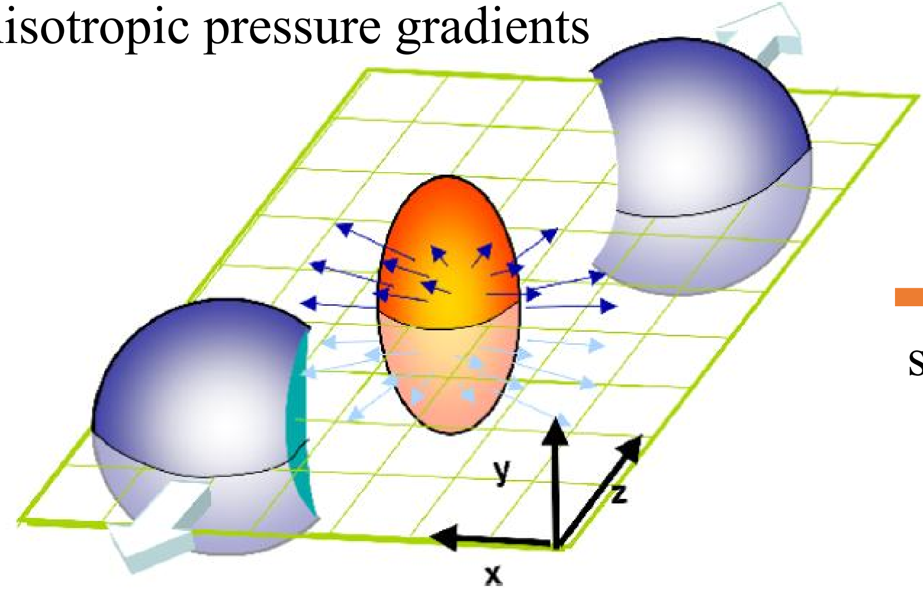

system expansion

anisotropic momentum distributions

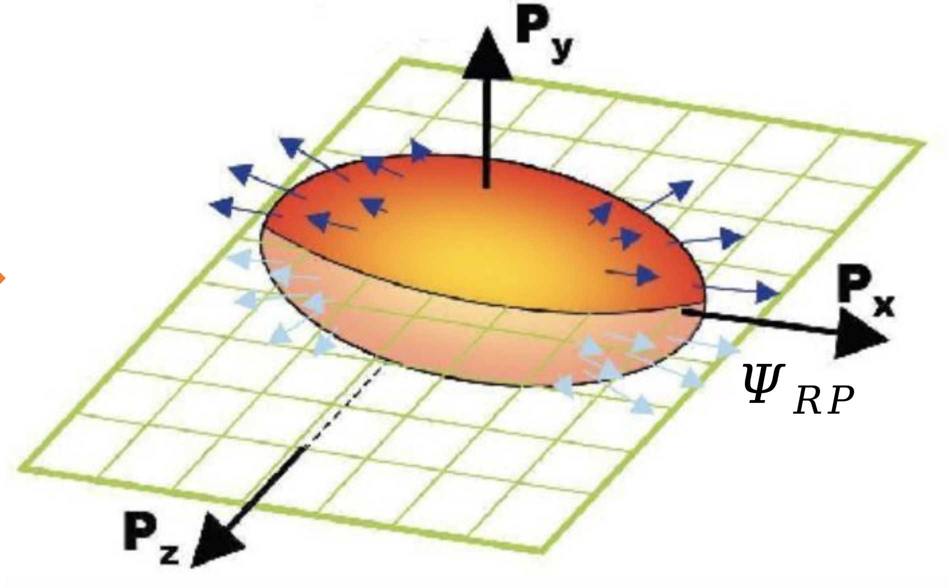

Initial state

$$\varepsilon_n = \frac{\sqrt{\langle r^n \cos(n\phi)\rangle^2 + \langle r^n \sin(n\phi)\rangle^2}}{\langle r^n \rangle}$$

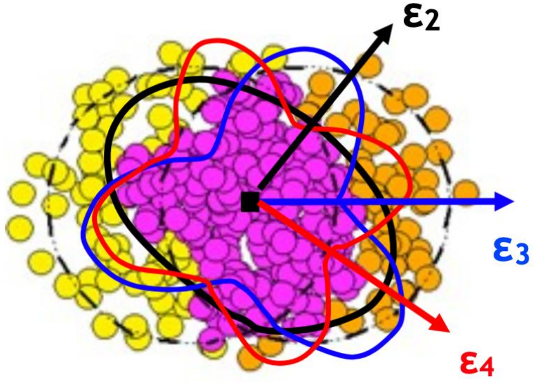

System expansion

Final state

$$\vec{V_n} = v_n\, e^{in\Psi_n}$$

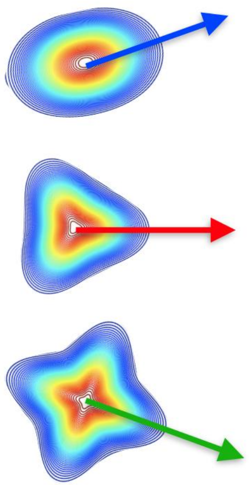

$\vec{V_2}$

$\vec{V_3}$

$\vec{V_4}$

$$\frac{dN}{d\varphi} \propto 1 + 2\sum_{n=1}^{\infty} v_n \cos n(\varphi - \Psi_n)$$

Fourier expansions

Anisotropic flow

Initial state

$$\varepsilon_n = \frac{\sqrt{\langle r^n \cos(n\phi)\rangle^2 + \langle r^n \sin(n\phi)\rangle^2}}{\langle r^n \rangle}$$

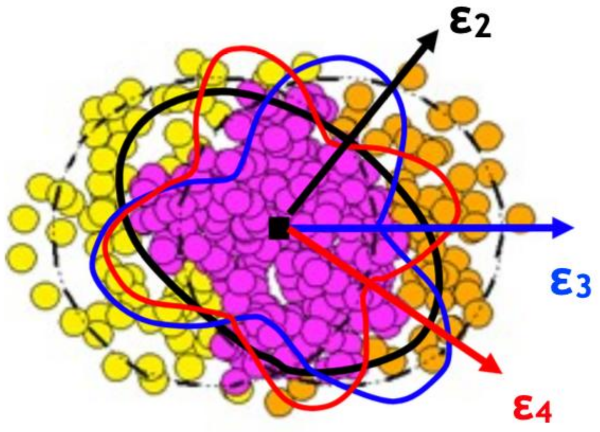

System expansion

Final state

$$\vec{V_n} = v_n\, e^{in\Psi_n}$$

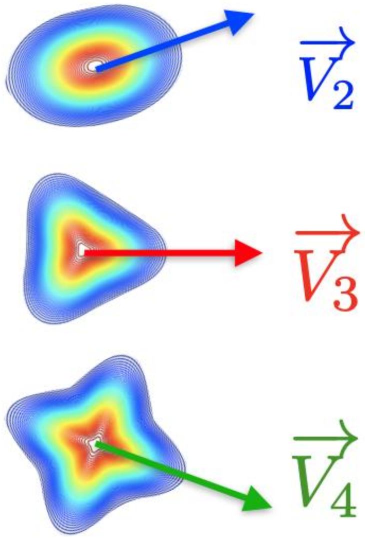

$$P(\varepsilon_m, \varepsilon_n, \varepsilon_k, ..., \Phi_m, \Phi_n, \Phi_k, ...) \Rightarrow P(v_m, v_n, v_k, ..., \Psi_m, \Psi_n, \Psi_k, ...)$$

How does v_n fluctuate	How does ψ_n fluctuate	How do v_n and v_m correlate	How do ψ_n and ψ_m correlate
$P(v_n)$	$P(\Psi_n)$	$P(v_m, v_n, v_k, ...)$	$P(\Psi_m, \Psi_n, \Psi_k, ...)$

Sensitivity in model

larger β_2

stronger initial geometric anisotropy (more elliptical)

stronger azimuthal anisotropy
larger v_2

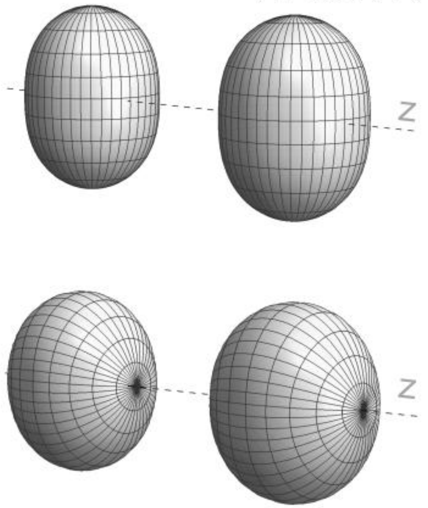

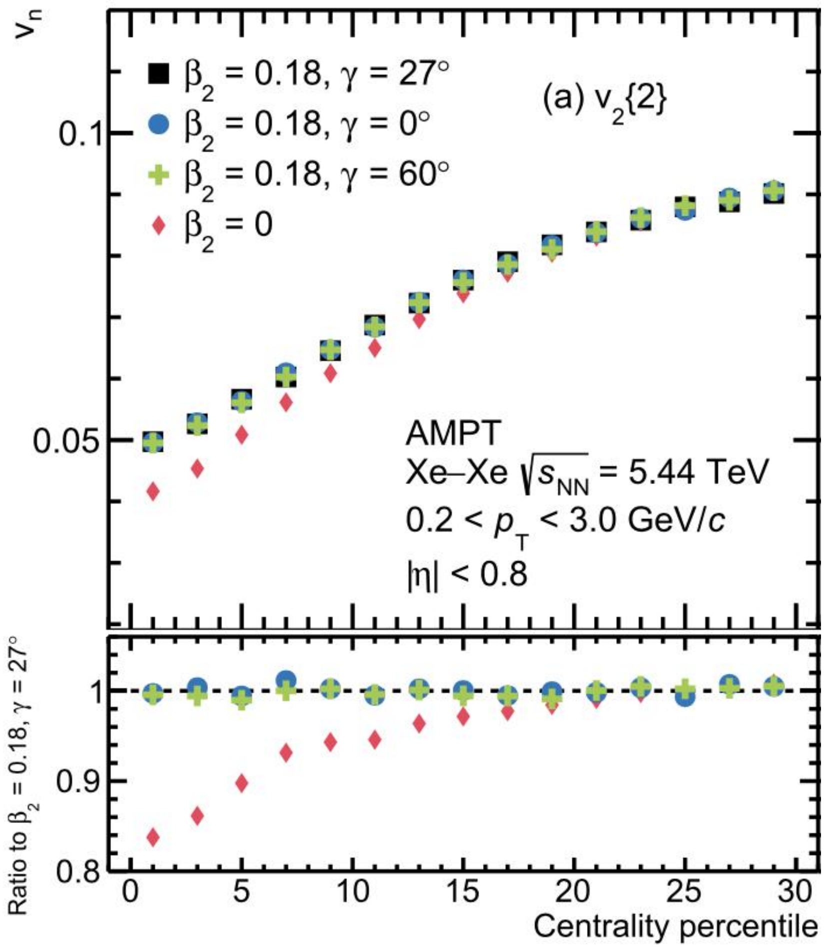

AMPT: Z. Lu et al., Eur. Phys. J. A 59 (2023) 279, arXiv:2309.09663

Sensitivity in model

larger a_0

more diffuse
larger initial size

smaller v_2

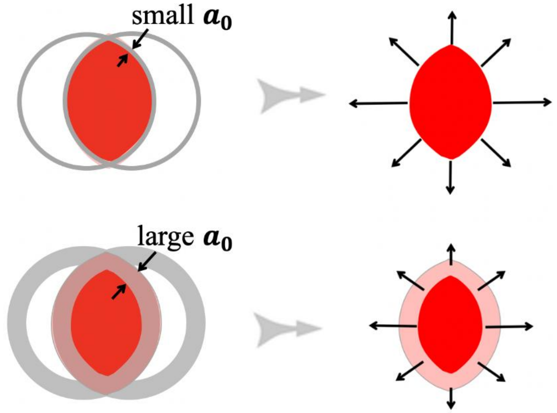

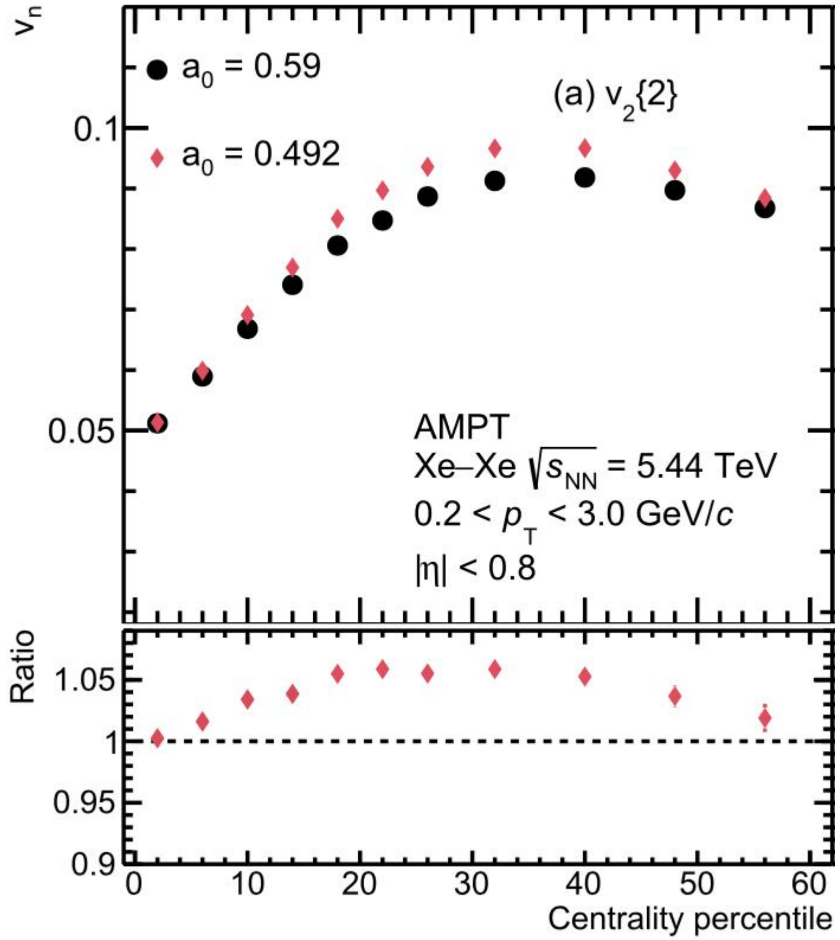

AMPT: Z. Lu et al., Eur. Phys. J. A 59 (2023) 279, arXiv:2309.09663

Sensitivity in model

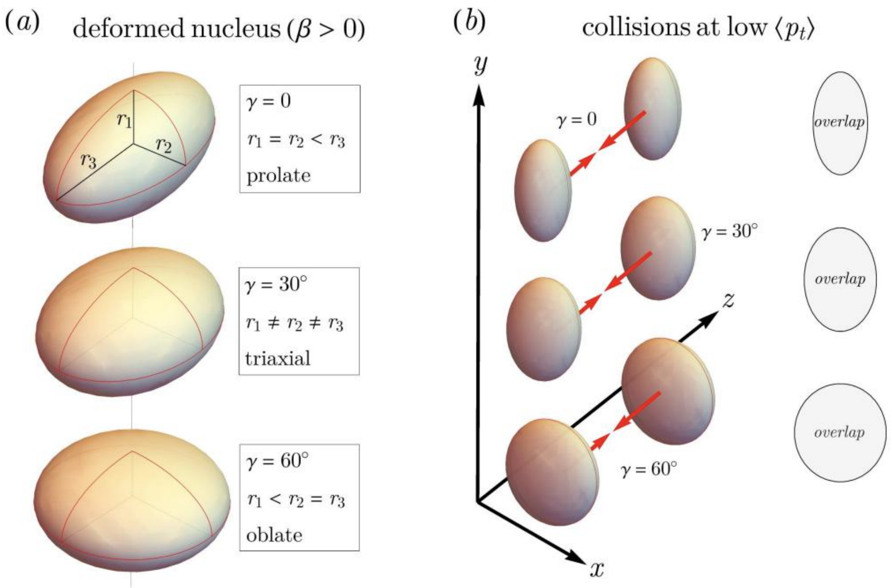

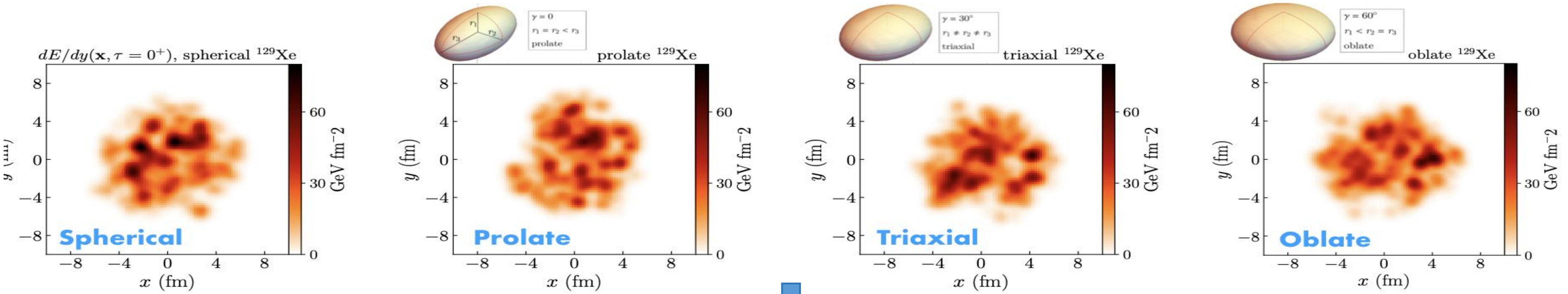

different azimuthal distributions of final-state particles

Probe nuclear deformation of ^{129}Xe with flow

ALICE, Physics Letters B 784 (2018) 82

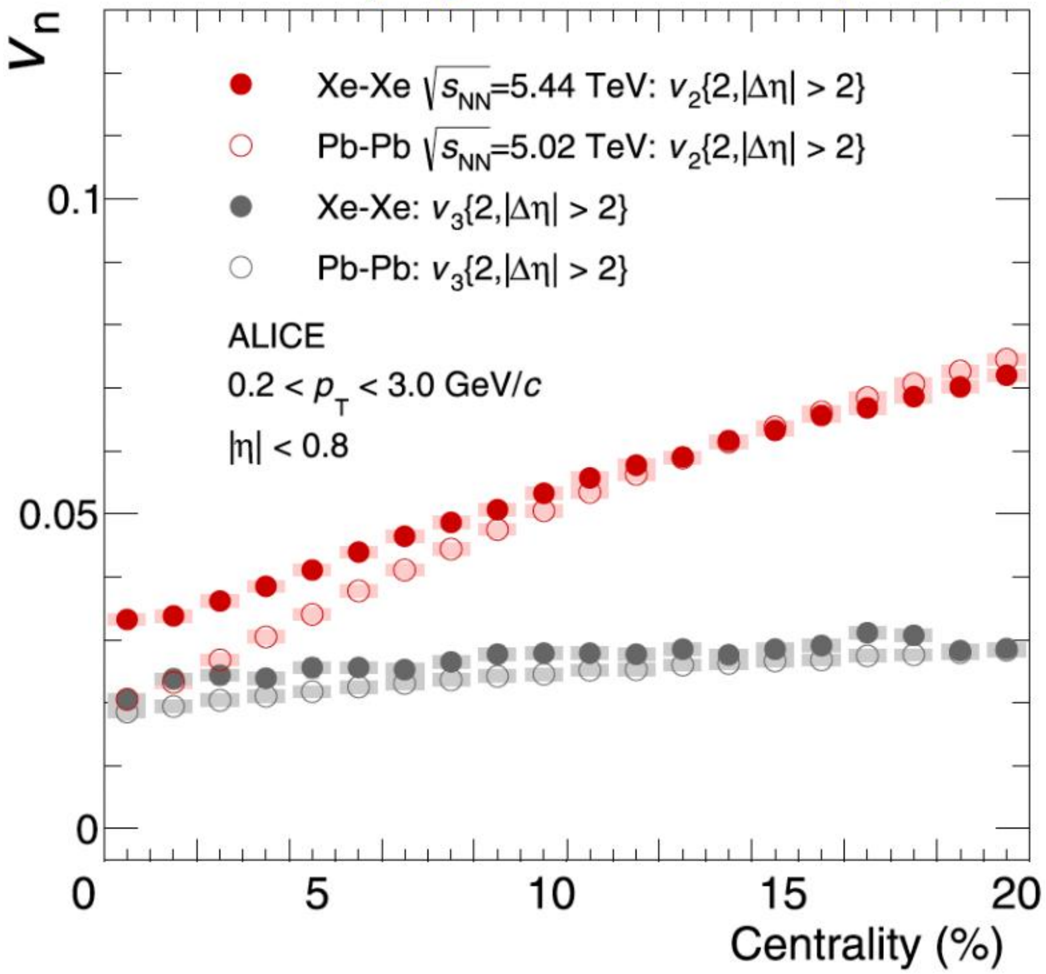

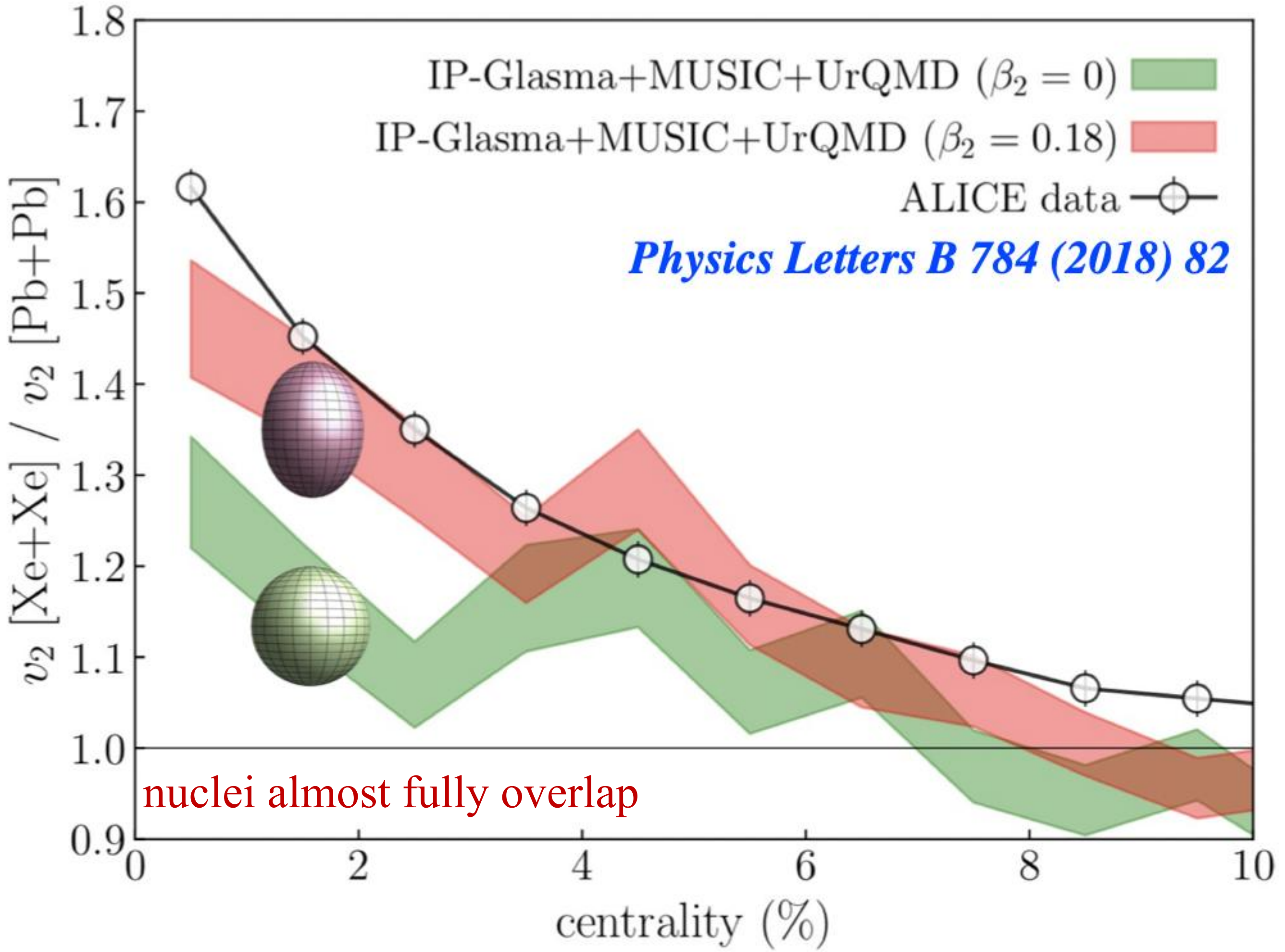

- Significant v_2 enhancements in central Xe-Xe collisions
- LHC data clearly suggests a non-zero β_2 (deformation of ^{129}Xe)

Probe nuclear deformation of ^{129}Xe with differential flow

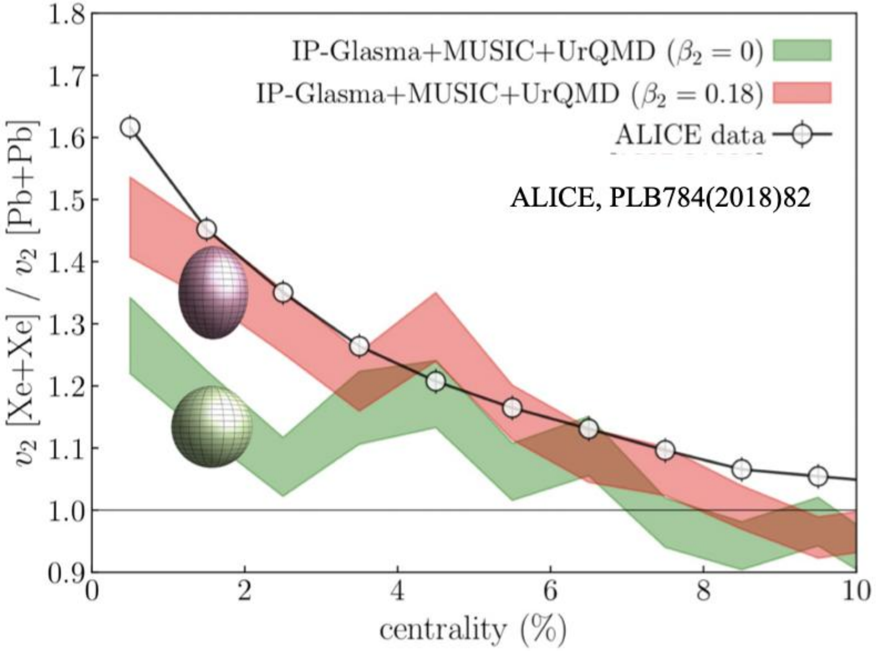

p_T-differential

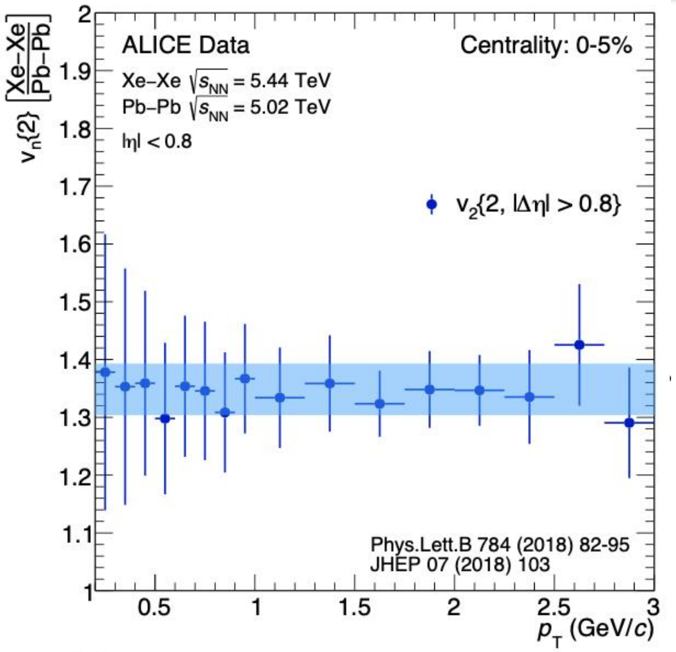

η-differential

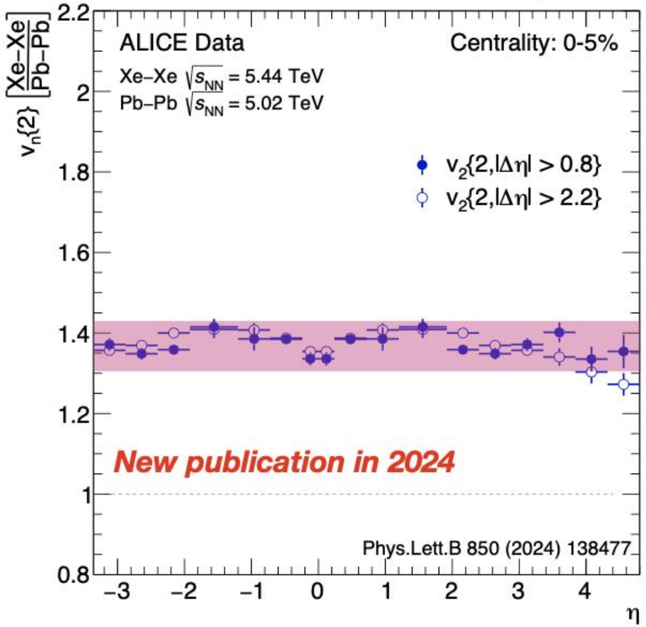

- For the first time observe the impact of NS over a very wide pseudorapidity range ($-3.5 < \eta < 5.0$)
- New input for the low-x physics (forward physics with large $|\eta|$)

Probe deformation of ^{129}Xe with $\Psi_n - \Psi_m$ correlation

$\rho_{422} \approx \langle \cos(4\Psi_4 - 4\Psi_2) \rangle$

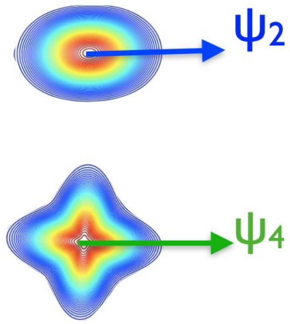

For Pb–Pb

Central collisions:

- Initial φ_2, φ_4 randomly fluctuate, weak correlations
- $\langle\cos 4(\psi_2-\psi_4)\rangle$ is small

Peripheral collisions:

- Initial φ_2, φ_4 tend to align, strong correlations
- $\langle\cos 4(\psi_2-\psi_4)\rangle$ is large

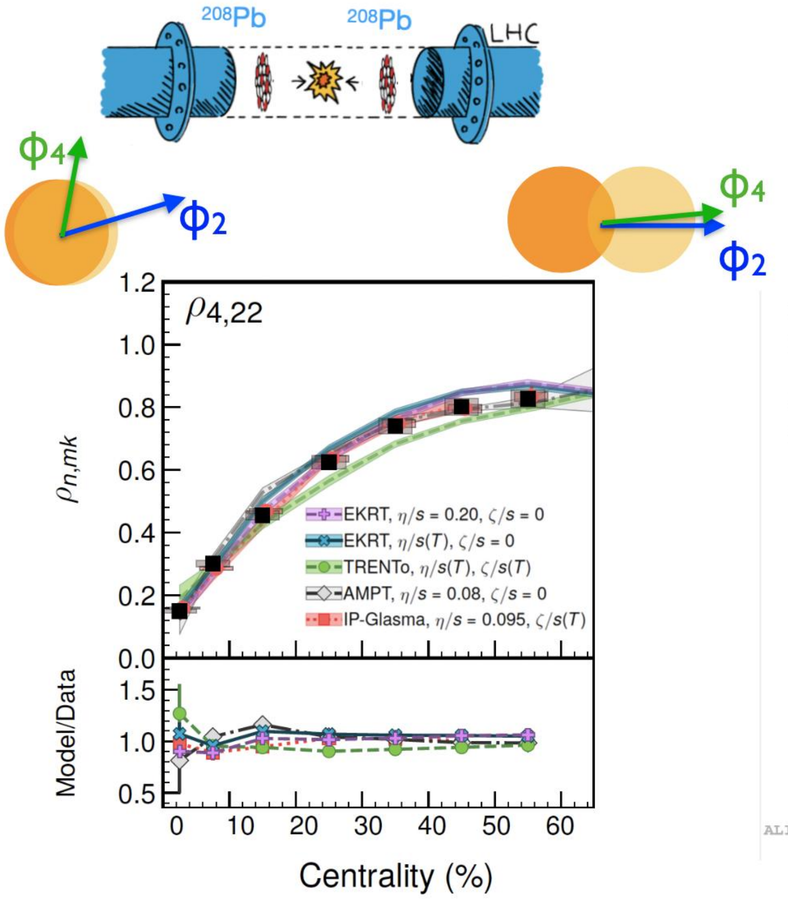

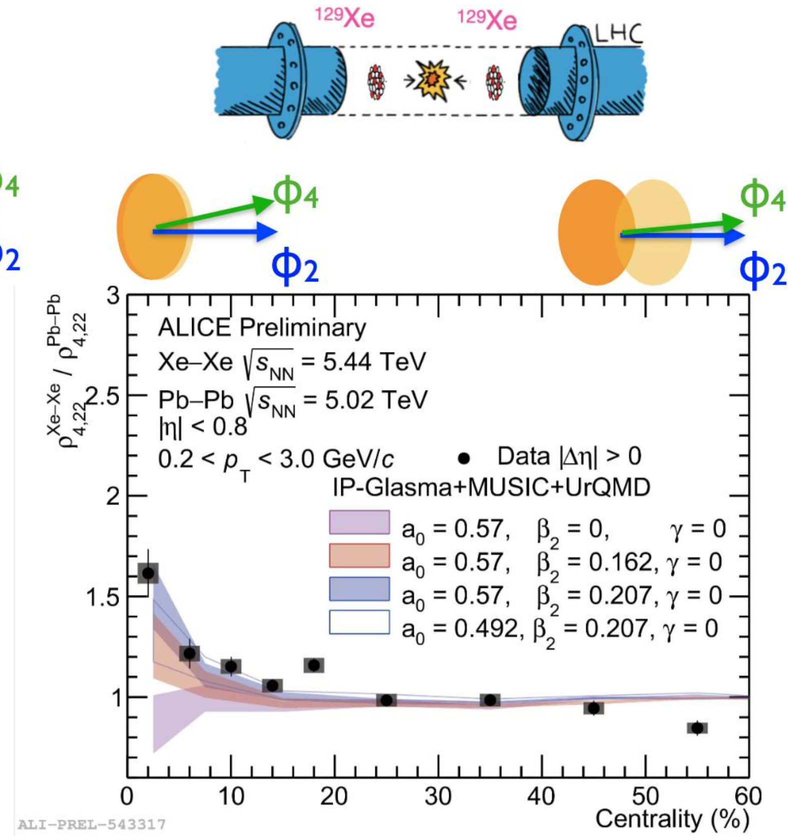

- A stronger correlation is observed in the Xe-Xe collisions because of deformation

Probe nuclear shape of ^{129}Xe with systematic flow studies

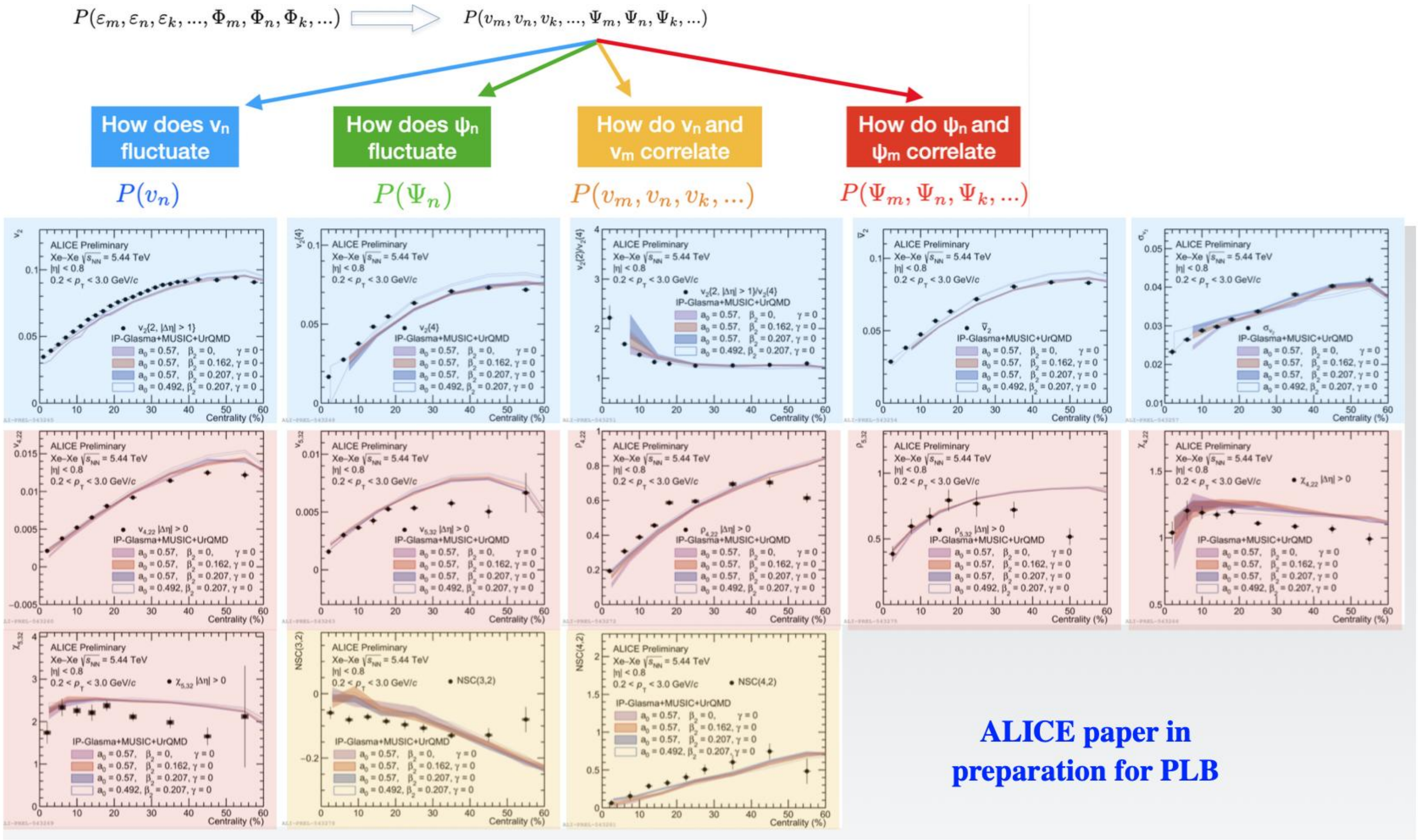

- Promising sensitivities to the nuclear deformation β_2 in central Xe-Xe collisions and nuclear skin a_0 in the mid-central collisions
- Insensitive to triaxial structure

Radial flow and $[p_T]$ correlation

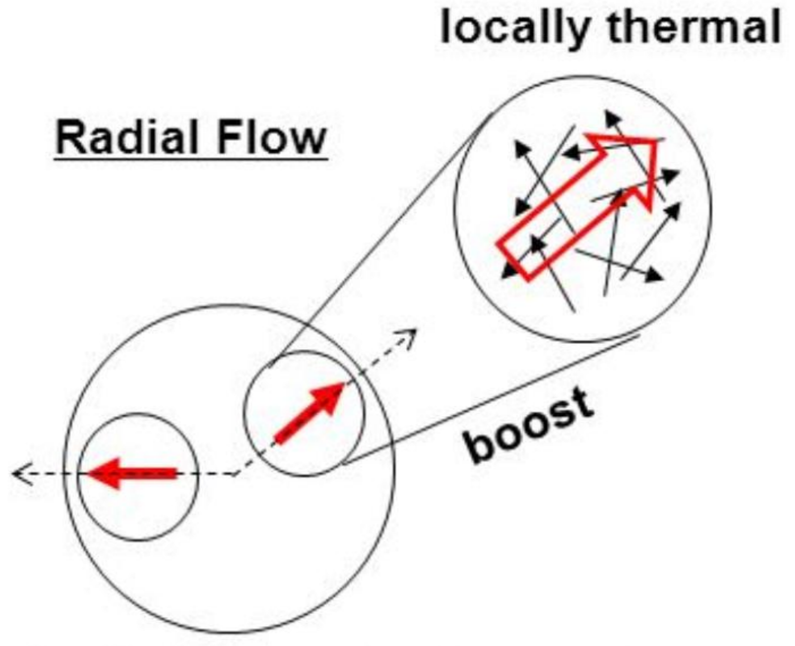

$$\frac{d\langle p_t\rangle}{\langle p_t\rangle} \propto \frac{dE}{E}$$

$$\frac{d\langle p_t\rangle}{\langle p_t\rangle} \propto -\frac{dR}{R}$$

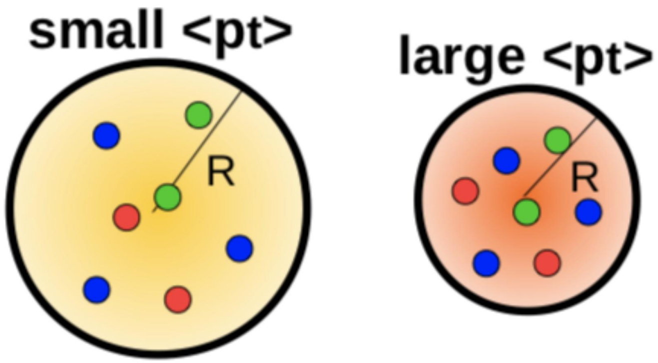

system expansion leads to an additional overall boost in momentum

Size of the QGP: radial flow, $[p_T]$

Radial flow and $[p_T]$ correlation

$$\frac{d\langle p_t\rangle}{\langle p_t\rangle} \propto \frac{dE}{E}$$

$$\frac{d\langle p_t\rangle}{\langle p_t\rangle} \propto -\frac{dR}{R}$$

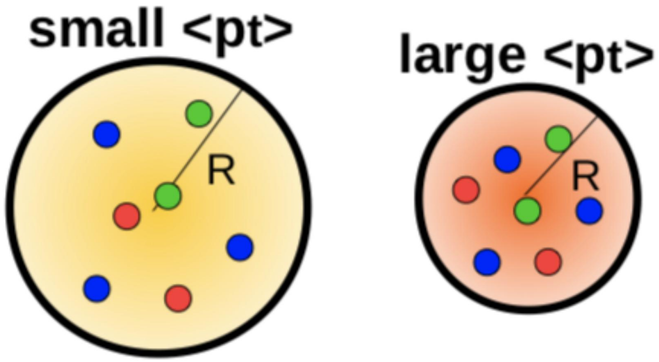

ALICE, PRC88 (2013) 044910, PRL111 (2013) 222301

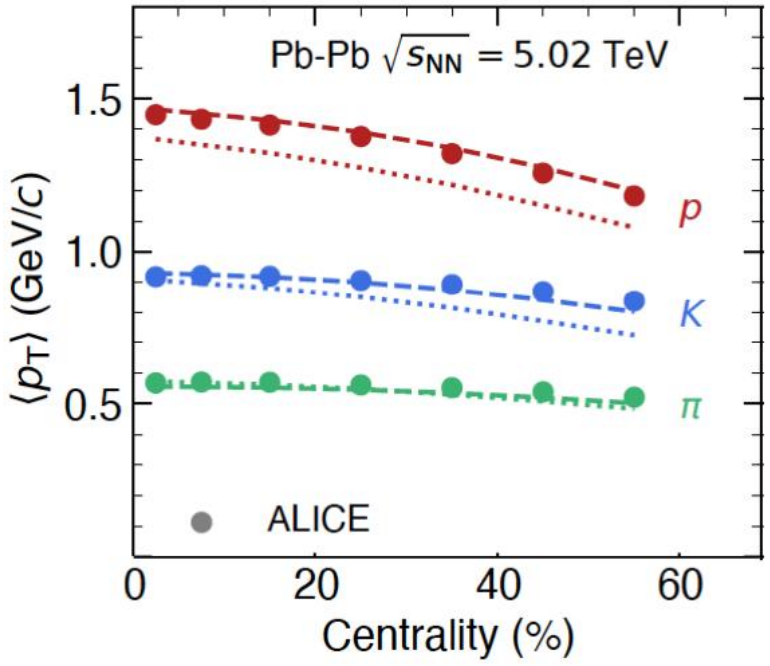

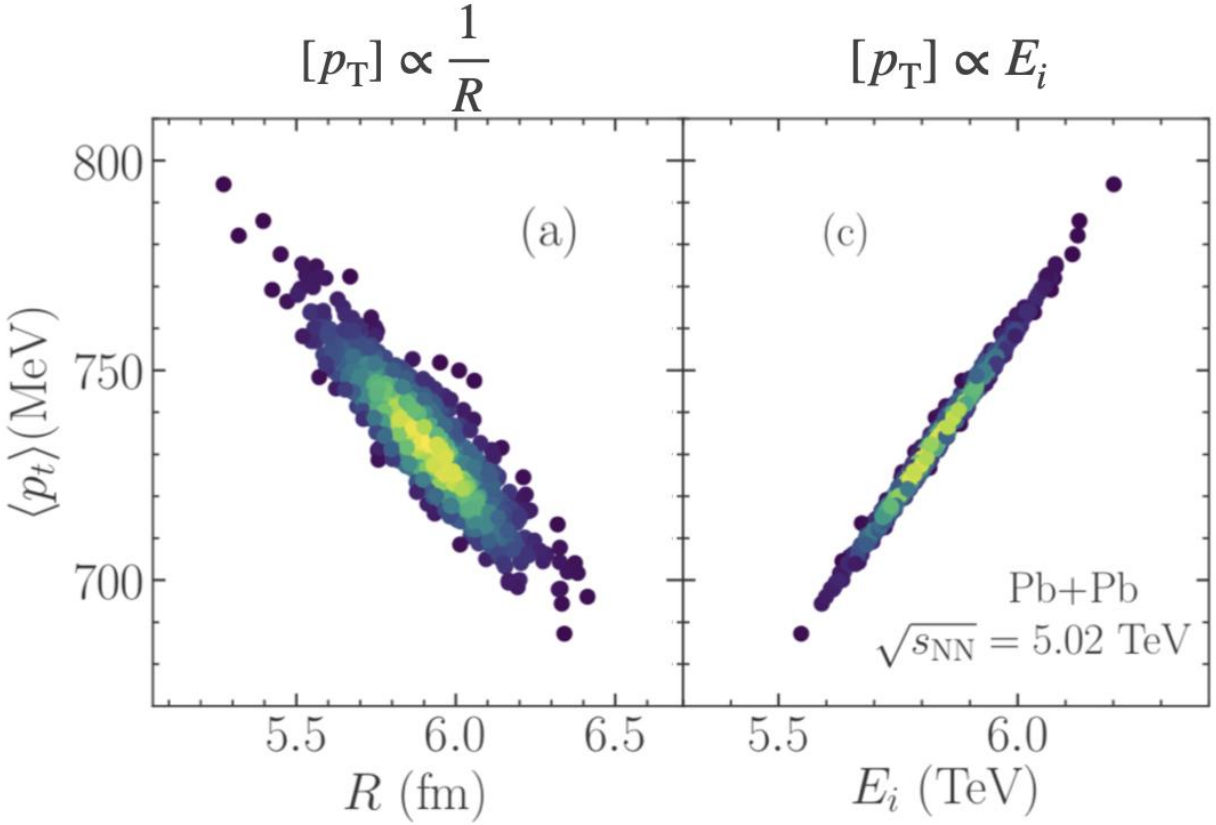

[G. Giacalone et al., PRC103 (2021) 2, 024909]

Radial flow and [p_T] correlation

❖ Multi-particle [p_T] correlations:

$$\langle p_T \rangle = \frac{\sum_{i=1}^{N_{ch}} p_{T,i}}{N_{ch}}$$

$$\langle \Delta p_{T,i} \Delta p_{T,j} \rangle = \left\langle \frac{\sum_{i,j,\, i\neq j}^{N_{ch}} (p_{T,i} - \langle\langle p_T \rangle\rangle)(p_{T,j} - \langle\langle p_T \rangle\rangle)}{N_{ch}(N_{ch}-1)} \right\rangle_{ev}$$

$$\langle \Delta p_{T,i} \Delta p_{T,j} \Delta p_{T,k} \rangle = \left\langle \frac{\sum_{i,j,k,\, i\neq j\neq k}^{N_{ch}} (p_{T,i} - \langle\langle p_T \rangle\rangle)(p_{T,j} - \langle\langle p_T \rangle\rangle)(p_{T,k} - \langle\langle p_T \rangle\rangle)}{N_{ch}(N_{ch}-1)(N_{ch}-2)} \right\rangle_{ev}$$

ALICE, EPJC 74 (2014) 3077

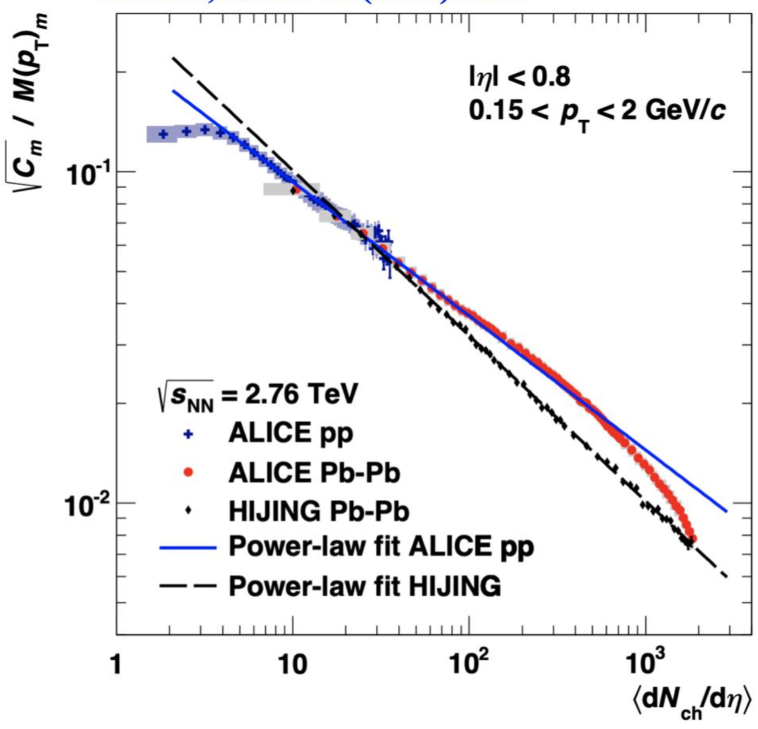

2nd-moment / 1st-moment

ALICE, PLB 850 (2024) 138541

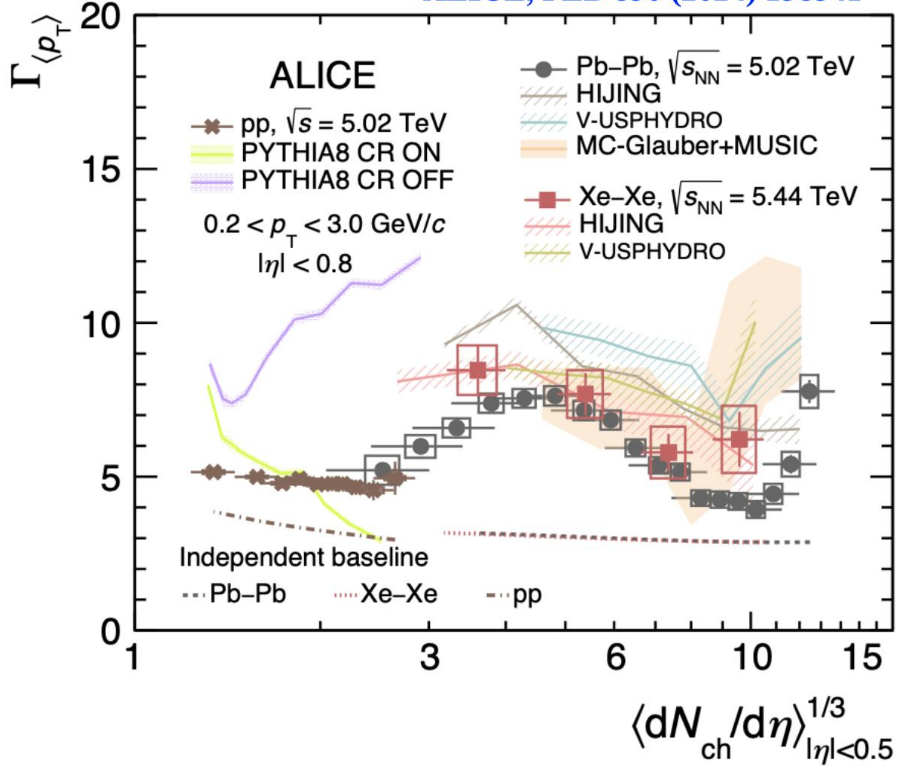

3rd-moment / 2nd-moment

[p_T] and its event-by-event fluctuations measured in heavy-ion collisions at the LHC
-> probe initial size and size fluctuations

Probe NS of ^{129}Xe with 2-particle $[p_T]$ correlation

$$[p_T^{(m)}] = \frac{\sum_{k_1 \neq \ldots \neq k_m}^{M} w_{k_1} \cdot \ldots \cdot w_{k_m} p_{T,k_1} \cdot \ldots \cdot p_{T,k_m}}{\sum_{k_1 \neq \ldots \neq k_m}^{M} w_{k_1} \cdot \ldots \cdot w_{k_m}},$$

$[p_T]$ cumulants in recursion formula:

$$\kappa_m = \langle [p_T^{(m)}] \rangle - \sum_{k=1}^{m-1} \binom{m-1}{k-1} \langle [p_T^{(m-k)}] \rangle \kappa_k.$$

Final state cumulant	Initial state cumulant	Liquid-drop model
κ_2	$\left\langle \left(\frac{\delta d_\perp}{d_\perp} \right)^2 \right\rangle$	$\frac{1}{32\pi} \langle \beta_2^2 \rangle$
κ_3	$\left\langle \left(\frac{\delta d_\perp}{d_\perp} \right)^3 \right\rangle$	$\frac{\sqrt{5}}{896\pi^{3/2}} \langle \cos(3\gamma) \beta_2^3 \rangle$

$$d_\perp = \sqrt{N_{\mathrm{part}} / \langle r_\perp^2 \rangle},$$

E. Nielsen etc., EPJA 60 (2024) 38

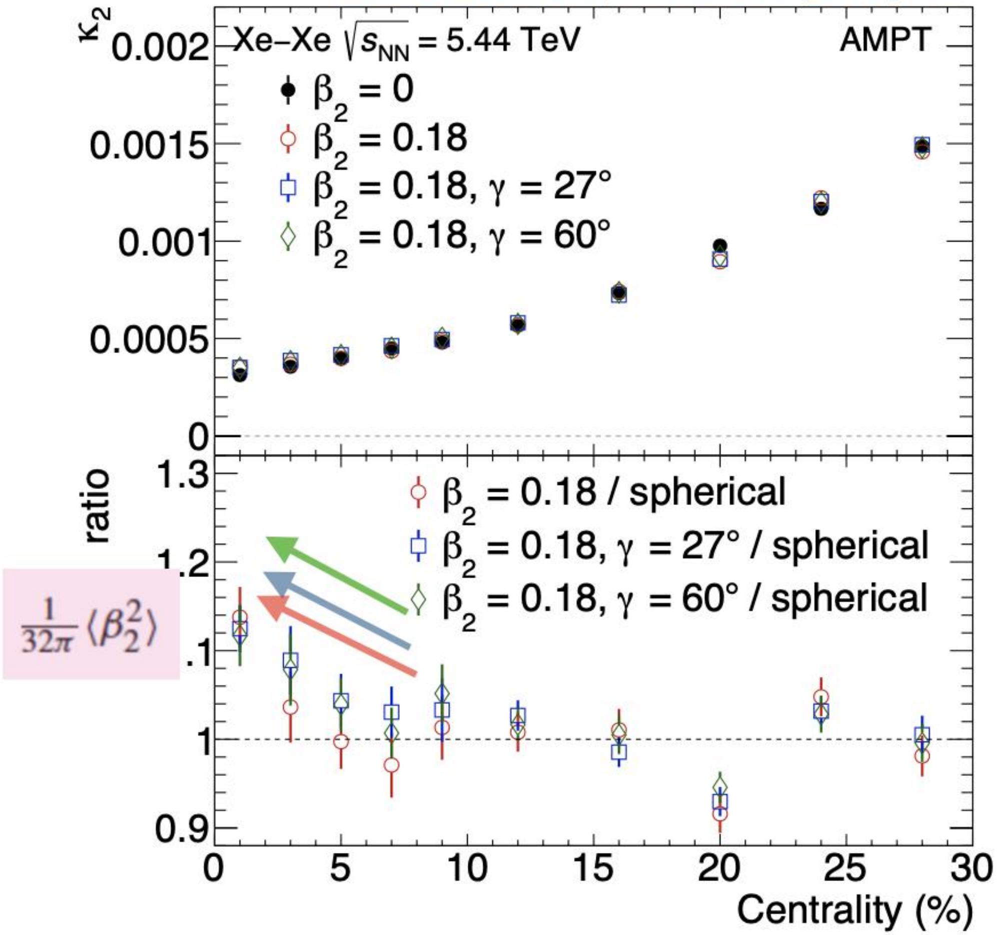

- These two-particle p_T correlations provide a new way to probe deformation structures of ^{129}Xe

Probe NS of ^{129}Xe with multi-particle $[p_T]$ correlation

$$[p_{\mathrm{T}}^{(m)}] = \frac{\sum\limits_{k_1 \neq \ldots \neq k_m}^{M} w_{k_1} \cdot \ldots \cdot w_{k_m} p_{\mathrm{T},k_1} \cdot \ldots \cdot p_{\mathrm{T},k_m}}{\sum\limits_{k_1 \neq \ldots \neq k_m}^{M} w_{k_1} \cdot \ldots \cdot w_{k_m}},$$

$$\kappa_m = \langle [p_{\mathrm{T}}^{(m)}] \rangle - \sum_{k=1}^{m-1} \binom{m-1}{k-1} \langle [p_{\mathrm{T}}^{(m-k)}] \rangle \kappa_k .$$

Final state cumulant	Initial state cumulant	Liquid-drop model
κ_2	$\left\langle \left(\frac{\delta d_\perp}{d_\perp} \right)^2 \right\rangle$	$\frac{1}{32\pi} \langle \beta_2^2 \rangle$
κ_3	$\left\langle \left(\frac{\delta d_\perp}{d_\perp} \right)^3 \right\rangle$	$\frac{\sqrt{5}}{896\pi^{3/2}} \langle \cos(3\gamma) \beta_2^3 \rangle$

$d_\perp = \sqrt{N_{\mathrm{part}}/\langle r_\perp^2 \rangle},$

- Multi-particle $[p_T]$ correlation reflects the initial size fluctuations, also bring new information on the triaxial structure.

E. Nielsen etc., EPJA 60 (2024) 38

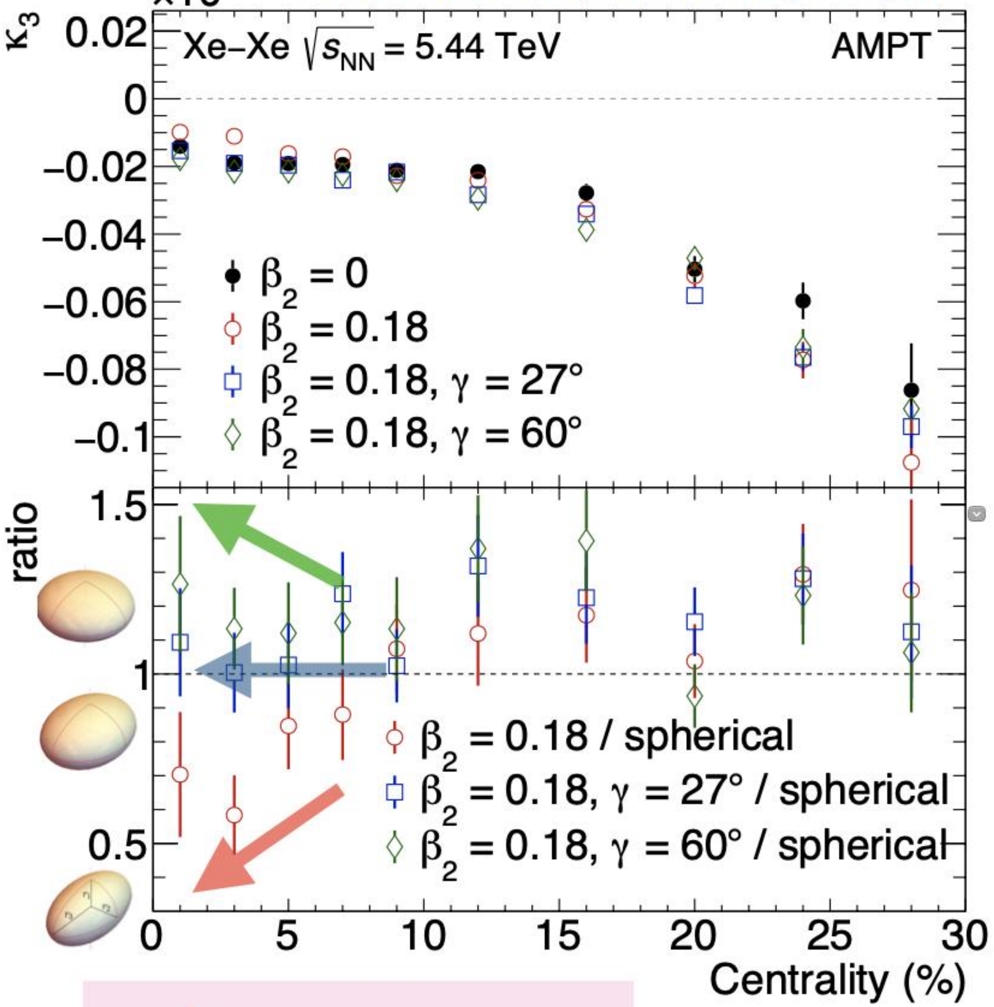

$$\frac{\sqrt{5}}{896\pi^{3/2}} \langle \cos(3\gamma) \beta_2^3 \rangle$$

v_n-$[p_T]$ correlations

Initial state $\varepsilon_n = \frac{\sqrt{\langle r^n \cos(n\phi)\rangle^2 + \langle r^n \sin(n\phi)\rangle^2}}{\langle r^n \rangle}$ Final state $\vec{V_n} = v_n e^{in\Psi_n}$

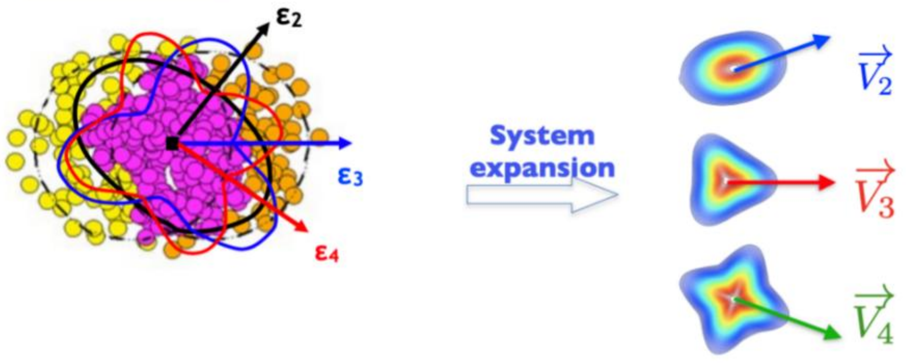

$P(\varepsilon_m, \varepsilon_n, \varepsilon_k, ..., \Phi_m, \Phi_n, \Phi_k, ...) \Rightarrow P(v_m, v_n, v_k, ..., \Psi_m, \Psi_n, \Psi_k, ...)$

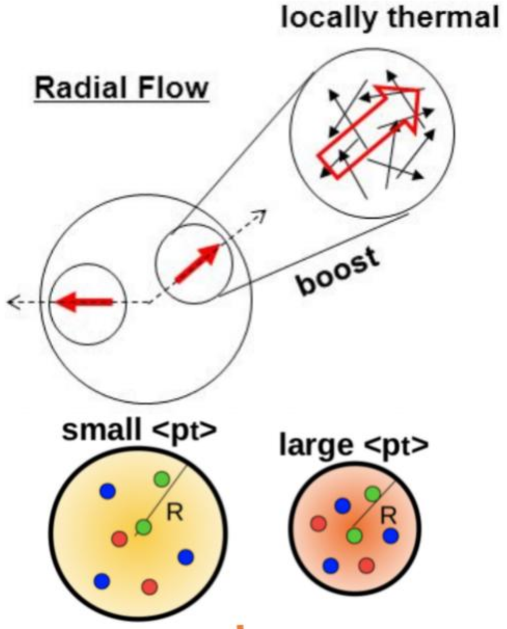

Experimental tools

How does v_n fluctuate	How does ψ_n fluctuate	How do v_n and v_m correlate	How do ψ_n and ψ_m correlate	$\langle p_T \rangle$ and its fluctuations
$P(v_n)$	$P(\Psi_n)$	$P(v_m, v_n, v_k, ...)$	$P(\Psi_m, \Psi_n, \Psi_k, ...)$	

vn-$\langle p_T \rangle$ correlations

Shape of the fireball: Anisotropic flow

Size of the fireball: radial flow, $[p_T]$

$$\rho(v_n^2, [p_T]) = \frac{cov(v_n^2, [p_T])}{\sqrt{var(v_n^2)}\sqrt{var([p_T])}}$$

Considering $v_n \propto \varepsilon_n$, $[p_T] \propto E_0$

$$\rho(v_n^2, [p_T]) = \rho(\varepsilon_n^2, [E_0])$$

final-state model calculation

Initial-state model estimation

P. Bozek etc, PRC96 (2017) 014904

Probe triaxial structure of ^{129}Xe

B. Bally etc, PRL128 (2022) 8, 082301

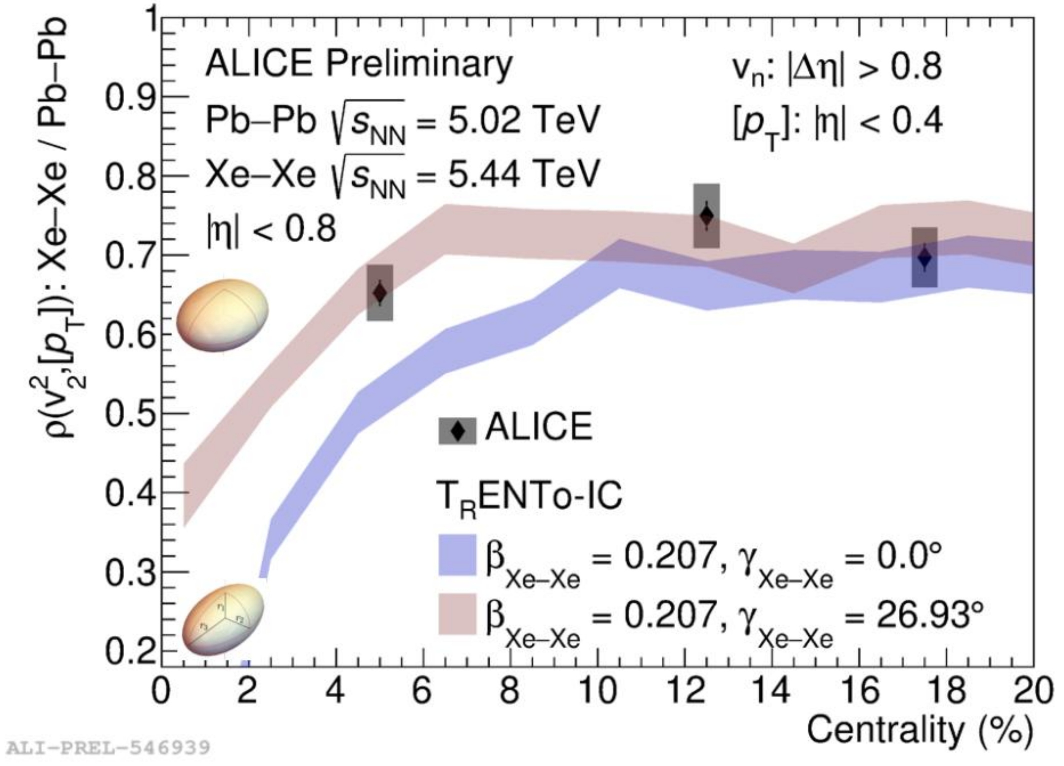

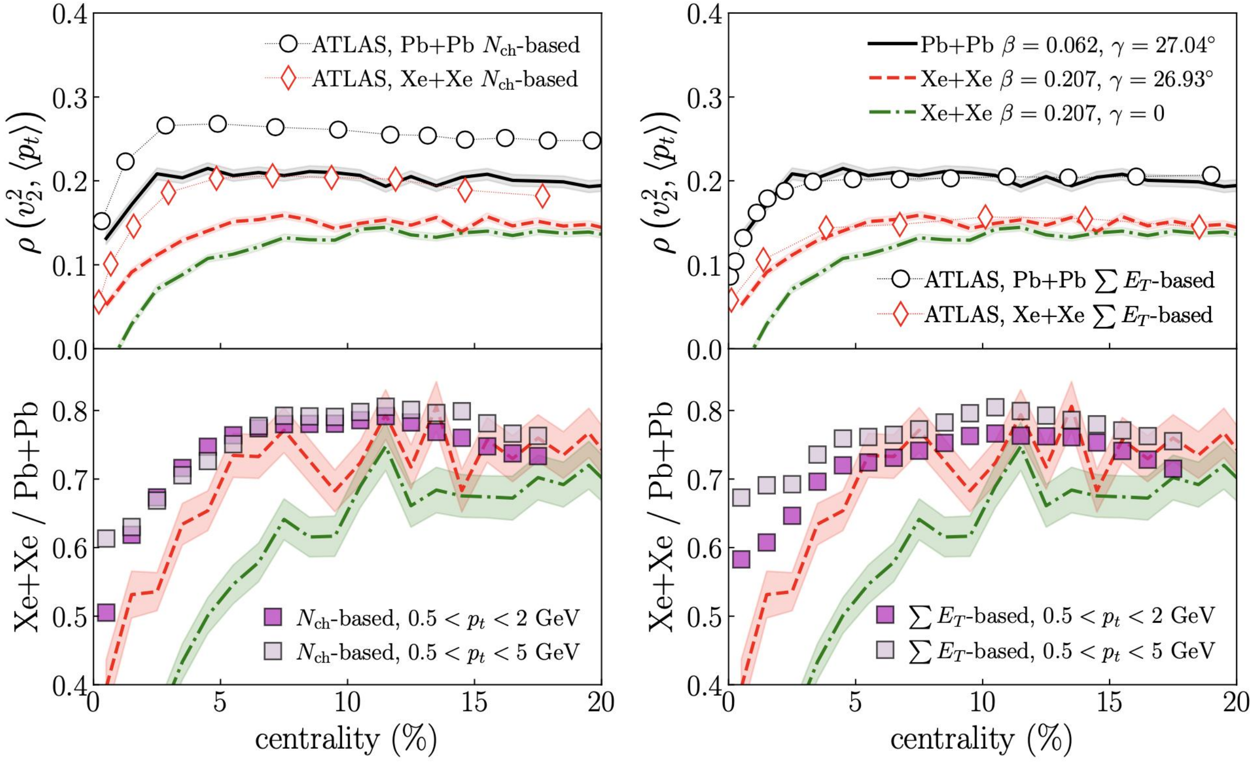

- "Standard" flow observables fail to probe γ (EPJA 59 (2023) 279)
- v_n–[p_T] correlations have significant sensitivities to γ
- Better agreement between LHC data and calculations with γ = 26.93°

Neutron skin of ^{208}Pb

PRL 131, 202302

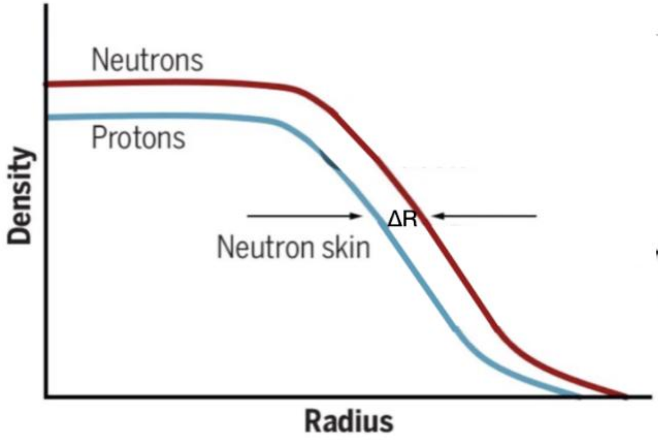

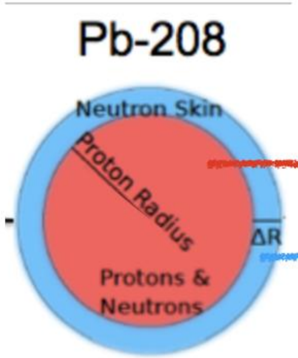

$$\rho(r,\Theta,\Phi) \propto \frac{1}{1+\exp\left(\left[r-R(\Theta,\Phi)\right]/a\right)}$$

$$\rho_p(r,\Theta,\Phi) \propto \frac{1}{1+\exp\left(\left[r_p-R_p(\Theta,\Phi)\right]/a_p\right)}$$

$$\rho_n(r,\Theta,\Phi) \propto \frac{1}{1+\exp\left(\left[r_n-R_n(\Theta,\Phi)\right]/a_n\right)}$$

a_p = 0.448 fm,
R_p = 6.680 fm,
r_p = 5.436 fm,
R_n = 6.690 fm

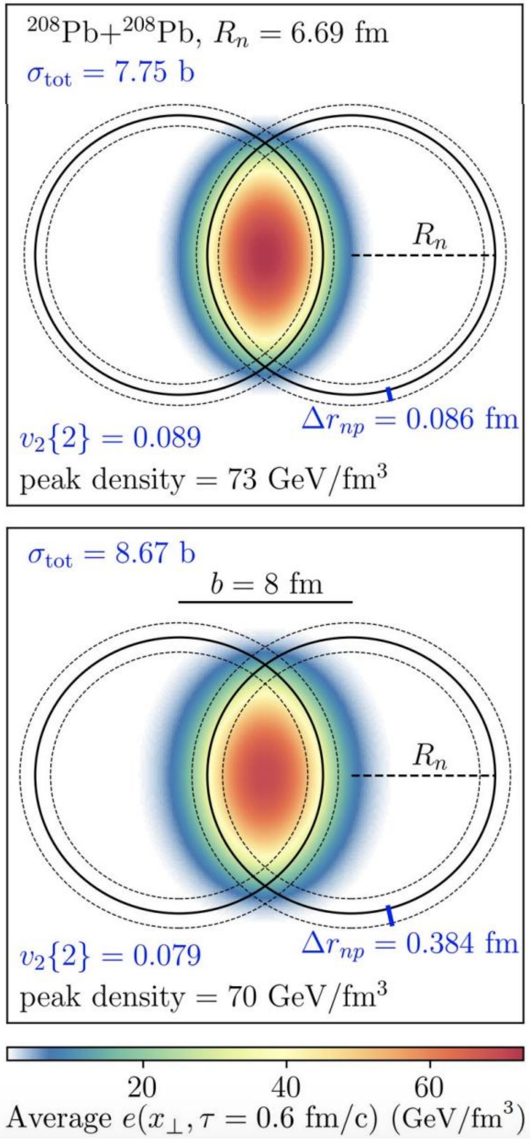

Large neutron skin → Large Initial size → Smaller [p_T] & stronger [p_T] fluctuations

Large Initial size → Weaker flow fluctuations

Extracting neutron skin of ^{208}Pb

CERN

Thick-skinned: Using heavy-ion collisions at the LHC, scientists determine the thickness of neutron “skin” in lead-208 nuclei

This is the first measurement of the neutron skin of lead-208 using exchanges predominantly involving gluons and it can provide insight into the structure of nuclei and neutron stars

15 NOVEMBER, 2023 | By Naomi Dinmore

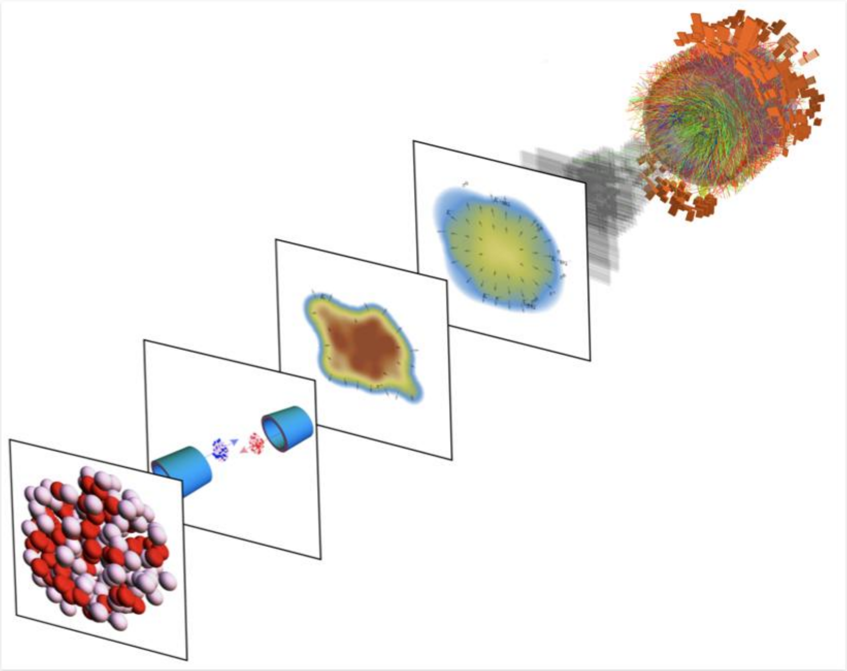

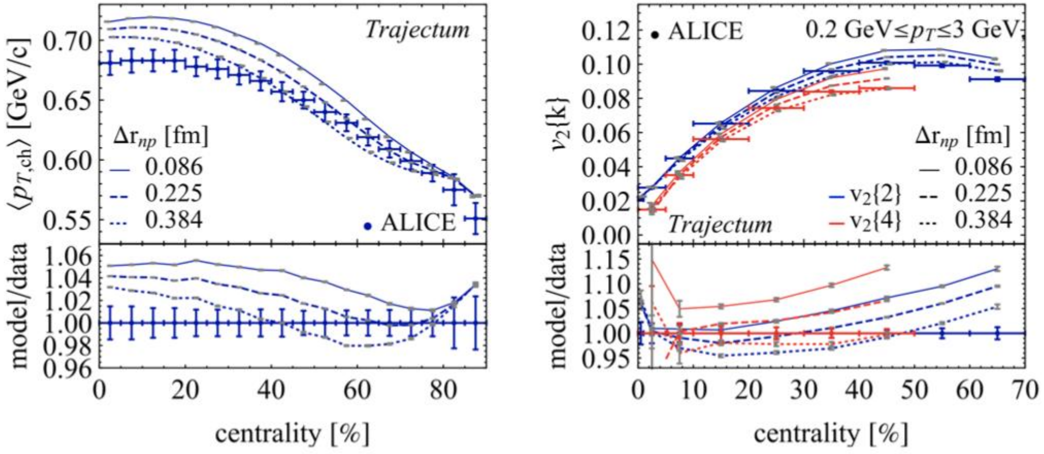

PRL131, 202302 (2023)

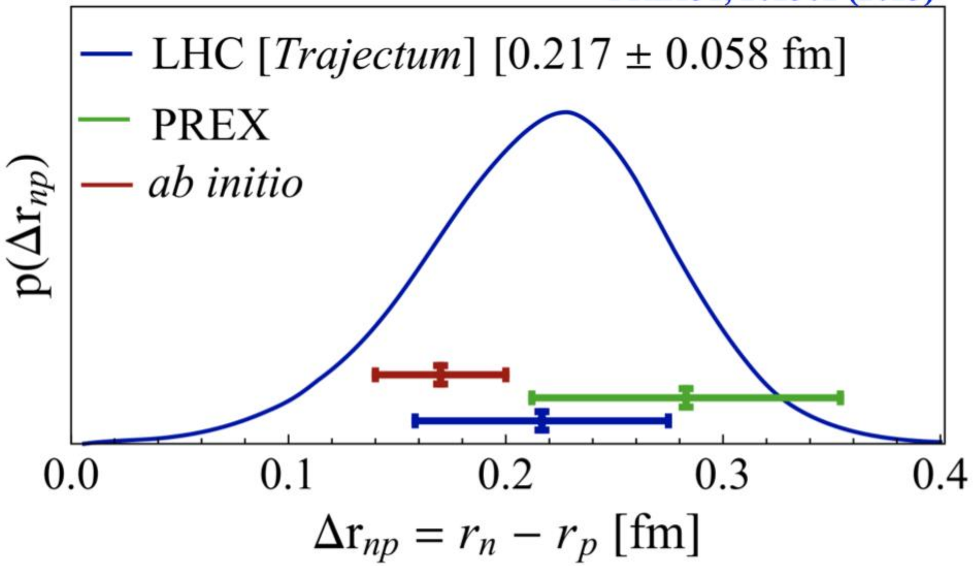

more applications at HIC

More than just flow and [p_T]

PHYSICAL REVIEW C

covering nuclear physics

Highlights Recent Accepted Collections Authors Referees Search Press About Editorial Tean

Open Access

Effect of initial nuclear deformation on dielectron photoproduction in hadronic heavy-ion collisions

Jiaxuan Luo, Xinbai Li, Zebo Tang, Xin Wu, and Wangmei Zha

Phys. Rev. C **108**, 054906 – Published 27 November 2023

arXiv > hep-ph > arXiv:2405.16491

Search..

Help

High Energy Physics – Phenomenology

[Submitted on 26 May 2024]

Nuclear deformation effects in photoproduction of ρ mesons in ultraperipheral isobaric collisions

Shuo Lin, Jin-Yu Hu, Hao-Jie Xu, Shi Pu, Qun Wang

Highlights

- ✓ **Experimental measurements at the RHIC/LHC enable a novel tool to probe the nuclear structure, complementary to the low-energy studies**

- **NS at low energies covers much wider range in the nuclide chart**
- **NS at high energies enables novel opportunity to resolve some challenging questions (many-body, shape etc) with a few selected nuclei**

Thanks for your attention!

Backup

Final state cancellation

Theorist:

- the cancellation can be seen in the PCC correlation between the initial state and final state
- Basically, the two systems have the same linear correlation between initial and final, which suggests the same final state effects.

$$Q_n = \frac{\langle v_n \varepsilon_n \cos n\left(\psi_n - \phi_n\right)\rangle}{\sqrt{\langle v_n^2\rangle\langle \varepsilon_n^2\rangle}}$$

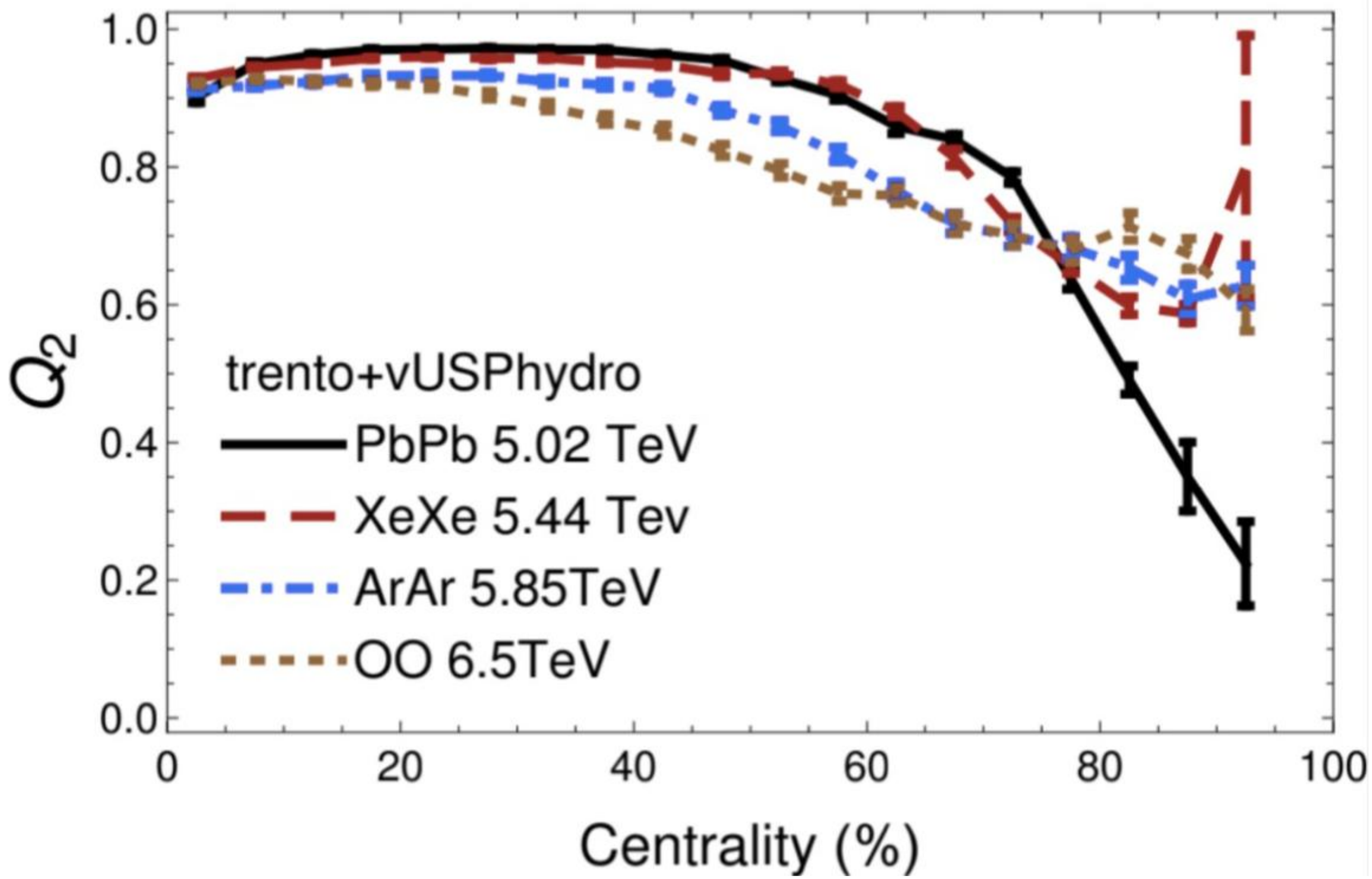

multi-particle [pT] correlation

Zhiyong Lu(CIAE)

$$d_\perp = \sqrt{N_{\text{part}}/\langle r_\perp^2\rangle}$$

$$\frac{\delta d_\perp}{d_\perp} = \sqrt{\frac{5}{16\pi}}\beta_2\Big(\cos(\gamma)D^2_{0,0}(\Omega) + \frac{\sin(\gamma)}{\sqrt{2}}[D^2_{0,2}(\Omega)+D^2_{0,-2}(\Omega)]\Big)$$

Final state cumulant	Initial state cumulant	Liquid-drop model
κ_2	$\left\langle\left(\frac{\delta d_\perp}{d_\perp}\right)^2\right\rangle$	$\frac{1}{32\pi}\langle\beta_2^2\rangle$
κ_3	$\left\langle\left(\frac{\delta d_\perp}{d_\perp}\right)^3\right\rangle$	$\frac{\sqrt{5}}{896\pi^{3/2}}\langle\cos(3\gamma)\beta_2^3\rangle$
κ_4	$\left\langle\left(\frac{\delta d_\perp}{d_\perp}\right)^4\right\rangle - 3\cdot\left\langle\left(\frac{\delta d_\perp}{d_\perp}\right)^2\right\rangle^2$	$-\frac{3}{14336\pi^2}(7\langle\beta_2^2\rangle - 5\langle\beta_2^4\rangle)$
κ_5	$\left\langle\left(\frac{\delta d_\perp}{d_\perp}\right)^5\right\rangle - 10\cdot\left\langle\left(\frac{\delta d_\perp}{d_\perp}\right)^3\right\rangle\cdot\left\langle\left(\frac{\delta d_\perp}{d_\perp}\right)^2\right\rangle$	$-\frac{5\sqrt{5}}{315392\pi^{5/2}}(11\langle\cos(3\gamma)\beta_2^3\rangle\langle\beta_2^2\rangle - 5\langle\beta_2^5\rangle)$
κ_6	$\left\langle\left(\frac{\delta d_\perp}{d_\perp}\right)^6\right\rangle - 15\cdot\left\langle\left(\frac{\delta d_\perp}{d_\perp}\right)^4\right\rangle\cdot\left\langle\left(\frac{\delta d_\perp}{d_\perp}\right)^2\right\rangle$ $+30\cdot\left\langle\left(\frac{\delta d_\perp}{d_\perp}\right)^2\right\rangle^3 - 10\cdot\left\langle\left(\frac{\delta d_\perp}{d_\perp}\right)^3\right\rangle^2$	$\frac{5}{918412504\pi^3}(42042\langle\beta_2^2\rangle^3 - 5720\langle\cos(3\gamma)\beta_2^3\rangle^2$ $-45045\langle\beta_2^2\rangle\langle\beta_2^4\rangle + 8575\langle\beta_2^6\rangle + 700\langle\cos(6\gamma)\beta_2^6\rangle)$
κ_7	$\left\langle\left(\frac{\delta d_\perp}{d_\perp}\right)^7\right\rangle - 21\cdot\left\langle\left(\frac{\delta d_\perp}{d_\perp}\right)^5\right\rangle\cdot\left\langle\left(\frac{\delta d_\perp}{d_\perp}\right)^2\right\rangle$ $+210\cdot\left\langle\left(\frac{\delta d_\perp}{d_\perp}\right)^3\right\rangle\cdot\left\langle\left(\frac{\delta d_\perp}{d_\perp}\right)^2\right\rangle^2$ $-35\cdot\left\langle\left(\frac{\delta d_\perp}{d_\perp}\right)^3\right\rangle\cdot\left\langle\left(\frac{\delta d_\perp}{d_\perp}\right)^4\right\rangle$	$-\frac{15\sqrt{5}}{524812288}(2002\langle\beta_2^2\rangle^2\langle\cos(3\gamma)\beta_2^3\rangle$ $+715\langle\cos(3\gamma)\beta_2^3\rangle\langle\beta_2^4\rangle$ $+910\langle\cos(3\gamma)\beta_2^5\rangle\langle\beta_2^2\rangle - 175\cos(3\gamma)\beta_2^7\rangle)$
κ_8	$\left\langle\left(\frac{\delta d_\perp}{d_\perp}\right)^8\right\rangle - 28\cdot\left\langle\left(\frac{\delta d_\perp}{d_\perp}\right)^6\right\rangle\cdot\left\langle\left(\frac{\delta d_\perp}{d_\perp}\right)^2\right\rangle$ $+420\cdot\left\langle\left(\frac{\delta d_\perp}{d_\perp}\right)^4\right\rangle\left\langle\left(\frac{\delta d_\perp}{d_\perp}\right)^2\right\rangle^2$ $-35\left\langle\left(\frac{\delta d_\perp}{d_\perp}\right)^4\right\rangle^2 - 630\cdot\left\langle\left(\frac{\delta d_\perp}{d_\perp}\right)^2\right\rangle^4$ $+560\cdot\left\langle\left(\frac{\delta d_\perp}{d_\perp}\right)^3\right\rangle^2\cdot\left\langle\left(\frac{\delta d_\perp}{d_\perp}\right)^2\right\rangle$ $-56\cdot\left\langle\left(\frac{\delta d_\perp}{d_\perp}\right)^5\right\rangle\cdot\left\langle\left(\frac{\delta d_\perp}{d_\perp}\right)^3\right\rangle$	$\frac{5}{142748942336\pi^4}(2144142\langle\beta_2^2\rangle^4 - 3063060\langle\beta_2^2\rangle^2\langle\beta_2^4\rangle$ $-340\langle\beta_2^2\rangle\Big(2288\langle\cos(3\gamma)\beta_2^3\rangle^2 - 35(49\langle\beta_2^6\rangle$ $+4\langle\cos(6\gamma)\beta_2^6\rangle)\Big) + 25\Big(21879\langle\beta_2^4\rangle^2$ $+14144\langle\cos(3\gamma)\beta_2^3\rangle\langle\cos(3\gamma)\beta_2^5\rangle$ $-35(79\langle\beta_2^8\rangle + 16\langle\cos(6\gamma)\beta_2^8\rangle)\Big)$

Zhiyong Lu(CIAE)

Enhanced ψn correlations in models

- ❖ $\rho_{4,22}$ probes correlations between Ψ_2 and Ψ_4 ~ $\langle \cos 4(\Psi_2 - \Psi_4) \rangle$

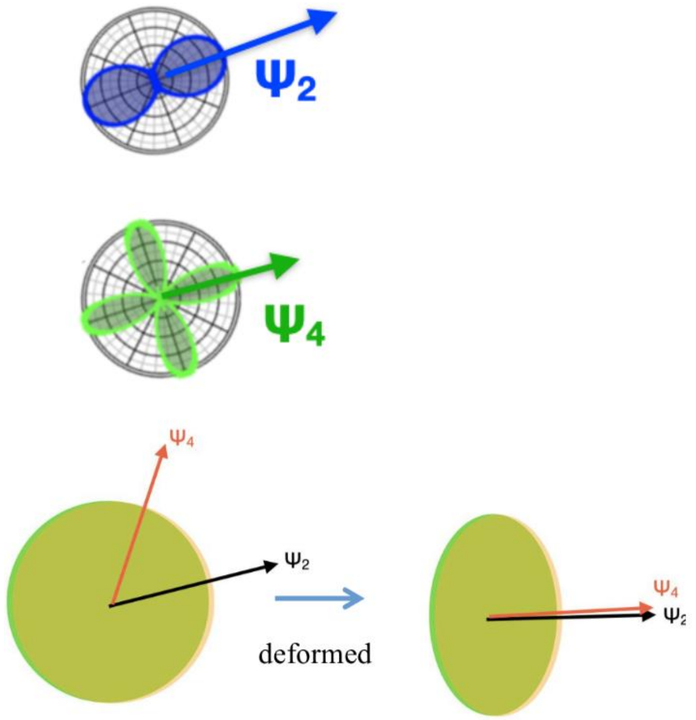

Z. Lu, M.Zhao, J. Jia, YZ, Eur. Phys. J. A (2023) 59, 279

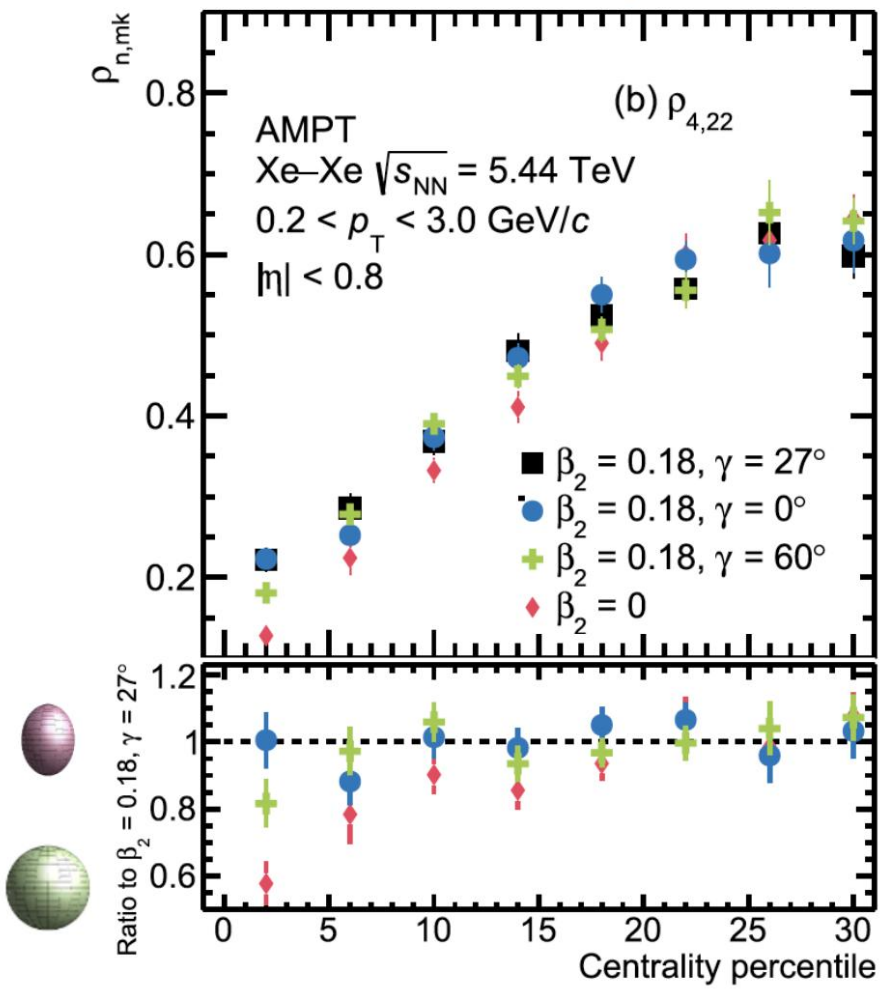

- ❖ A stronger correlation is well explained by the transport model using deformed ^{129}Xe nuclei using transport model

Status of vn-[pT] studies